Journal of Nonlinear Modeling and Analysis
Volume 7, Number 3, June 2025, 997–1036
https://journal.global-sci.org/jnma
DOI:10.12150/jnma.2025.997

The Fractal-Fractional Mathematical Model Analysis of the Impact of HIV/AIDS on the Working-Class in Ethiopia

Abdulsamad Engida Sado[1,†], Gemechis File Duressa[2] and Chernet Tuge Deressa[2]

Abstract The HIV/AIDS epidemic profoundly affects the working-class population, resulting in increased mortality and morbidity rates and causing substantial labour loss across various sectors. To assess the epidemic's impact on the specified class, a fractal-fractional-order mathematical model was formulated based on Atangana-Baleanu-Caputo operator. This model encompasses seven compartments, and the existence and uniqueness of its solutions were verified based on the Banach fixed-point theorem, contraction mapping concepts, and Hyers-Ulam stability criteria. The mathematical model was analyzed to understand the effects of HIV/AIDS on the working-class population. Real data from Ethiopia were utilized to validate the model. Subsequently, the model was extended to optimal control fractal-fractional models, incorporating different control strategies. Numerical simulations were performed using MATLAB R2019a to support the analytical solutions. The study's results demonstrated that the fractal-fractional-order model provides a comprehensive understanding of the complexities of HIV/AIDS infection. The findings suggested that increasing the number of infected productive members of the population can help to control the spread of the disease by reducing the inequality caused by HIV/AIDS. Furthermore, the numerical simulation of the optimal control model indicated that decreasing non-productivity reduces the number of infected individuals. Therefore, effective management of the infection holds the potential to eradicate the disease in the country.

Keywords Hyers-Ulam stability, HIV/AIDS, working-class population, optimal-control, fractional order, fractal-fractional

MSC(2010) 39B82, 92D30, 49J15, 34A08, 28A80

1. Introduction

The human immunodeficiency virus (HIV) affects approximately 39.9 million individuals worldwide, and the sub-Saharan African region bears a disproportionate share of this disease burden. Ethiopia, a sub-Saharan nation, grapples with this HIV/AIDS crisis Kanki et al. [1]. Developing robust behavioral change and educational initiatives at the community level is pivotal for mitigating the prevalence of

[†]the corresponding author.
Email address:abdulsemede@gmail.com(Abdulsamad E.), gammeef@gmail.com(Gemechis F.),chernet.deressa@ju.edu.et(Chernet T,)
[1]Mathematics, Debre Berhan University, Debra Berhan, Ahmara, Ethiopia
[2]Mathematics, Jimma University, Jimma, Oromia, Ethiopia

prejudice and stigma against people living with HIV/AIDS (PLWHA) Arefaynie et al. [2]. The human immunodeficiency virus (HIV) undermines the immune system, leading to acquired immunodeficiency syndrome (AIDS), which can be transmitted through unprotected sexual intercourse, shared drug injection equipment, or from mother to child during childbirth or breastfeeding. Preventive strategies encompass consistent condom usage, routine testing and counseling, timely initiation and follow-up of antiretroviral therapy (ART), pre-exposure prophylaxis (PrEP), and measures to avert mother-to-child transmission [3, 4].

The HIV/AIDS crisis intersects with COVID-19 and exacerbates numerous problems for those living with and infected by the disease. People living with HIV/AIDS demand a comprehensive global response to this pandemic. Troubling new data from the UNAIDS global AIDS update of 2023 portend a grim outlook, as progress has stagnated, resources have dwindled, and inequities have intensified. The global population of individuals living with HIV increased from 38 million in 2020 to 38.4 million in 2021 during the COVID-19 pandemic and 39.9 million in 2023, with the African region accounting for 67% of these cases. HIV-affected populations have also grown in the Middle East and North Africa. Maintaining the current trajectory will result in millions of additional HIV infections and AIDS-related deaths [5]. Therefore, further investigation and research on HIV/AIDS are imperative to re-examine the nature of the pandemic and its effects on productive forces and other community groups. If left uncontrolled, HIV/AIDS infection will continue to pose a grave public health and economic challenge worldwide [6, 7]. Global efforts must focus on raising awareness, eliminating stigma, and addressing the socioeconomic factors that contribute to the endemic nature of this crisis. Ongoing research and public health initiatives are essential in the fight against HIV/AIDS Shiferaw et al. [3]. The lack of comprehensive data on behavioral trends in Ethiopia hinders the accurate interpretation of HIV prevalence and incidence, obscuring a clear understanding of the current state of the HIV/AIDS epidemic in the country Adal [8].

Fractional calculus encompasses the study of non-integer order derivatives [9, 10]. It is employed to describe a typical diffusion process that can influence our understanding of disease transmission in unconventional ways. This domain of research is relatively well-developed in fields such as physics and engineering, and its application to infectious disease modeling remains an emerging area of inquiry. It is crucial to note that the utilization of mathematical models for infectious diseases with a fractal-fractional order model is employed to capture the intricacy and self-similarity of disease transmission models. The spatial distribution of infections, or temporal patterns of epidemic waves, can exhibit fractal-like characteristics Abu and Saadeh [11]. This approach is valuable for capturing the heterogeneity and irregularity of real systems, providing a more comprehensive understanding of the spatial and temporal dynamics of diseases. The Atangana-Baleanu operator of fractional calculus in the sense of Caputo is a specialized operator of fractional calculus introduced to extend the classical Caputo fractional operator Atangana [12]. Fractional operators are mathematical tools that generalize the concept of derivatives and integrals to non-integer orders, enabling a more precise description of various phenomena, particularly those related to memory and distance dependence [10, 13–16]. Atangana and Baleanu introduced this fractional operator in their work on fractional calculus and integral transformations of generalized functions to provide an alternative approach to fractional calculus that incorporates the Caputo meaning and considers certain related restrictions. The Atangana-Baleanu operator

of the fractional order is particularly useful in situations where the standard Caputo fractional derivative is challenging, such as when singularities are present or when dealing with functions of different derivative orders.

Recently, distinctive differentiation operators have been created by combining the concepts of fractional order and fractal dimension. Novel operators were constructed utilizing three kernels: power law, exponential decay, and the extended Mittag-Leffler function. The fractional order and fractal dimension are two parameters related to the new operator fractal-fractional order differential equations [17,18]. The selection of the fractal-fractional operator depends on the special properties of the model system and the mathematical properties desired in the analysis Atangana [19]. The fractional-order differential equation operator has been applied to epidemiology models by different researchers [20–23], and the fractal-fractional order has been employed to model diseases such as Influenza, Tuberculosis, the 2019-nCoV pandemic, COVID-19, Hepatitis C virus, Malaria, Ebola, Alzheimer's disease, tumor growth and many other infectious diseases, as discussed by various researchers [24–32]. Additionally, fractal- fractional order has been applied in numerous other areas of physics, engineering, and information science [33–39].

Differential calculus is known to present difficulties when it comes to solving nonlinear equations. Since the fractional model addresses the issue of nonlocal and nonlinear, it is not easy to provide practical accurate solutions for these systems. As a result, the investigation of the existence and uniqueness of solutions for the fractional model is our main concern. We use the fixed-point theorem to achieve this. The Ulam-Hyers approach provides a crucial viewpoint of the dependence on initial values and useful in assessing the system's stability [18,40]. However, because it is challenging to obtain precise solutions for these models using current analytical methods, numerical solutions are required in order to assess the effectiveness of such fractal-fractional operators in modeling solutions. We shall approximate the Atangana-Baleanu fractional integral using the numerical approach newly developed by Toufik et al [41] and the fractal-fractional model using the methods of Atangana and Qureshi [42]. This computing method integrates the concepts of fractional calculus with the two-step Lagrange polynomial interpolation method. This technique has proven remarkably accurate and effective. It is renowned for being very easy to use and for accelerating the convergence to the exact solution, especially when dealing with large discretization steps. Various mathematical epidemiology studies adopted the numerical methods [43, 44].

A mathematical analysis of an industrial HIV/AIDS or mass workplace model that incorporates a carefree attitude toward the sex of the labor force was performed by integral order model. Depending on this related model the researcher modify and incorporated pre-AIDS stages of the disease by removing free sex attitude Seidu and Makinde [45]. In this study, we aimed to investigate the impact of HIV/AIDS on the working-class population using fractal-fractional order mathematical modeling techniques. Our goal was to gain a comprehensive understanding of the complexity of HIV/AIDS within the working-class population. Furthermore, we analyze the Atangana-Baleanu-Caputo fractional-order and fractal-dimensional perspectives within mathematical modeling frameworks. Fractal-fractional-based models provide a balance between accuracy and computational tractability in capturing dynamic systems with uncertainty. Some hospital-recorded data and state variables in our study may not align with specific parameters; thus, we estimated parameters from existing data. Therefore, users of this study need to take into ac-

count this limitation. The manuscript is structured as follows: The fractal-fractional calculus, mathematical modeling formulations, as well as the construction and analysis of mathematical models, are covered in Section 2. The results of the numerical simulation and parameter estimates are presented in Section 3. Section 4 discusses the model's extension to the optimal control and numerical simulation. Section 5 provides a brief conclusion.

2. Model formulation and analysis

We formulated a fractional-order model using the Atangana-Baleanu-Caputo (ABC) operator and extended it to a fractal-fractional model for HIV/AIDS in Ethiopia's working-class population.

2.1. Definition and preliminary concepts

To formulate the fractional-order Atangana-Baleanu operators used for the model in Equation (2.1), we must replace the ordinary derivatives with the corresponding fractional derivatives. The fractional order Atangana-Baleanu derivative in the Caputo sense is defined as follows Atangana [12].

Definition 2.1. Let $f(t) \in W_2^1(0,l)$. Then, for $\omega \in [0,1]$, the Atangana- Baleanu fractional derivative in the Caputo sense of function $f(t)$ is given by

$$ {}_{a}^{ABC}D_t^{\omega} f(t) = \frac{ABC(\omega)}{1-\omega} \int_a^t \frac{d}{d\tau} f(\tau) E_{\omega} \left[\frac{-\omega}{1-\omega} (t-\tau)^{\omega} \right] d\tau, $$

where the special function $ABC(0) = ABC(1) = 1$ and E_ω is the Mittag-Leffler function.

Definition 2.2. The Atangana-Baleanu fractional integral of the function $f(t)$ is defined as follows:

$$ {}_{a}^{ABC}I_t^{\omega}[f(t)] = \frac{1-\omega}{ABC(\omega)} f(t) + \frac{\omega}{ABC(\omega)\Gamma(\omega)} \int_a^t f(\tau)(t-\tau)^{\omega-1} d\tau. $$

where Γ is the gamma function, and E_α is the Mittag-Leffler function as Atangana [12].

Definition 2.3. Let f(t) be differentiable in the open interval (a, b); if f is fractionally differentiable on (a,b) with order ω, then the fractal-fractional derivative of dimension ϱ in the Atangana-Baleanu fractional derivative in the Caputo sense is given as

$$ {}^{ABC}D^{\omega,\varrho}(f(t)) = \frac{ABC(\omega)}{1-\omega} \frac{d}{d\tau^{\varrho}} \int_0^t f(\tau) E_{\omega}[-\frac{\omega}{1-\omega}(t-\tau\omega)^{\omega}] d\tau. $$

Definition 2.4. Following Atangana [19], consider a continuous function $f(t)$ in (a,b) with fractional order $0 < \omega \leq 1$ and fractal dimension $0 < \varrho \leq 1$, which can be defined in the ABC sense as:

$$ {}^{ABC}I_0^{\omega} t(f(t)) = \frac{1-\omega}{ABC(\omega)} t^{\varrho-1} f(t) + \frac{\omega\varrho}{ABC(\omega)\Gamma(\omega)} \int_0^t s^{\varrho-1}(t-\tau)^{\omega-1} f(\tau) d\tau, $$

where $ABC(0) = ABC(1) = 1$ is called the normalization constant [12, 46].

Definition 2.5. As Gómez and Atangana [18] let us define the solution for the given problem as $0 < \omega \leq 1$ and $0 < \varrho \leq 1$

$$^{ABC}D^{\omega} f(t) = \varrho t^{\varrho-1}\mathcal{F}(t, f(t)), t \in [0, T],$$
$$f(t) = f_0, 0 < \omega \leq 1, 0 < \varrho \leq 1,$$

provided by

$$f(t) = f_0 + \frac{1-\omega}{ABC(\omega)}\varrho t^{\varrho-1}\mathcal{F}(t, f(t)) + \frac{\omega\varrho}{ABC(\omega)\Gamma(\omega)}\int_0^t \tau^{\varrho-1}(t-\tau)^{\omega-1}\mathcal{F}(\tau, f(\tau))d\tau.$$

2.2. Fractional-order model formulation and analysis

In this section, an Atangana-Baleanu-Caputo-based fractional order model of HIV/AIDS based on a working-class population in Ethiopia is developed. The model has seven compartments, each of them represents a distinct class of people within the working-class population. The components are as follows: (S_p^*) susceptible productive people who are HIV-negative and capable of doing their jobs well; (S_n^*) susceptible nonproductive people, who do not have HIV and nonproductive; (I_p^*) Productive infected persons with HIV, who can work well while not having AIDS symptoms; (I_n^*) HIV positive nonproductive people, who have the virus but do not exhibit signs of AIDS, which raises their risk of infection and lowers their production; (A_{pp}^*) people who were productive pre-AIDS epidemic but who currently have HIV and certain AIDS symptoms and can work; (A_{pn}^*) pre-AIDS nonproductive people, those with HIV infection who have shown certain signs of the disease and nonproductive; and (A^*) Full-blown AIDS patients, those with HIV infection who have severe symptoms of the disease and are unable to work. As soon as the person in compartment I_p^*, I_n^* realizes that they have HIV, they begin therapy. Next, they proceed to (A_{pp}^*) and (A_{pn}^*), based on the stage of the cluster of differentiation cell count level(CD4).

The force of infection $\Lambda = \beta^* \frac{I_p^* + I_n^* + A_{pp}^* + A_{pn}^*}{N}$; and all other parameters included in the model to represent various rates of infection, recruitment, progression, mortality, and modification parameters are described in Table 1. The model is described by a system of seven nonlinear fractional-order Atangana-Baleanu-Caputo operator differential equations, which represent the changes in the sizes of each compartment over time. The system is given by the following flow diagram Figure 1.

The governing dynamical system in the ABC fractional operator is given in Equation (2.1).

Table 1. Parameter Descriptions and Values

Parameter	Description	Values	Sources
Q^*	Rate of recruitment	0.5	Scaled
π^*	Fraction of new recruits in the S_p^* class	0.5	Estimated
$1-\pi^*$	Fraction of new recruits in the S_n^* class	0.5	Calculated
σ_1^*	Rate at which nonproductive susceptibles become Productive	0.020	Fitted
σ_2^*	Rate at which nonproductive pre-AIDS become productive	0.020	Fitted
θ^*	Rate at which nonproductive infected become productive	0.0012	Fitted
β^*	Contact rate between susceptibles and infectives	0.0201	Fitted
$\tau^* > 1$	Modification parameter due to nonproductive behavior of susceptibles	1.3	Estimated
δ_1^*	Rate of progression of I_p^* class into pre-AIDS	0.0036	Fitted
δ_2^*	Rate of progression of I_n^* class into pre-AIDS non-productive	0.0014	Fitted
k	Natural death rate	0.0148	Calculated
ψ^*	AIDS-induced death rate	0.1	Estimated
k_1^*	Rate of progression of the A_{pp}^* class into A^*	0.007	Fitted
k_2^*	Rate of progression of the A_{pn}^* class into A^*	0.0012	Fitted

$$
\begin{aligned}
{}_0^{ABC}D_t^{\omega} S_p^* &= \pi^* Q^* + \sigma_1^* S_n^* - (\Lambda+\kappa) S_p^*,\\
{}_0^{ABC}D_t^{\omega} S_n^* &= (1-\pi^*) Q^* - (\tau^*\Lambda + \sigma_1^* + \kappa) S_n^*,\\
{}_0^{ABC}D_t^{\omega} I_p^* &= \Lambda S_p^* + \theta^* I_n^* - (\delta_1^* + \kappa) I_p^*,\\
{}_0^{ABC}D_t^{\omega} I_n^* &= \tau^*\Lambda S_n^* - (\theta^* + \delta_2^* + \kappa) I_n^*,\\
{}_0^{ABC}D_t^{\omega} A_{pp}^* &= \delta_1^* I_p^* + \sigma_2^* A_{pn}^* - (k_1^* + \kappa) A_{pp}^*,\\
{}_0^{ABC}D_t^{\omega} A_{pn}^* &= \delta_2^* I_n^* - (\sigma_2^* + k_2^* + \kappa) A_{pn}^*,\\
{}_0^{ABC}D_t^{\omega} A^* &= k_1^* A_{pp}^* + k_2^* A_{pn}^* - (\kappa + \psi^*) A^*.
\end{aligned}
\tag{2.1}
$$

with the initial conditions $S_p^*(0) > 0, S_n^*(0) > 0, I_p^*(0) > 0, I_n^*(0) > 0, A_{pp}^*(0) > 0, A_{pn}^*(0) > 0, A^*(0) > 0$, where all the initial values are positive. The system is a commensurate fractional-order system because all the systems have the same fractional order (ω).

2.3. Fractal-fractional representation with the ABC-operator model

The fractional-order model based on the ABC of Equation (2.1) is extended to a Atangana-Baleanu-Caputo fractal-fractional denoted as (ABF) model with Caputo with time dimension of ϱ and fractional-order ω; for more, see [19,46] and references

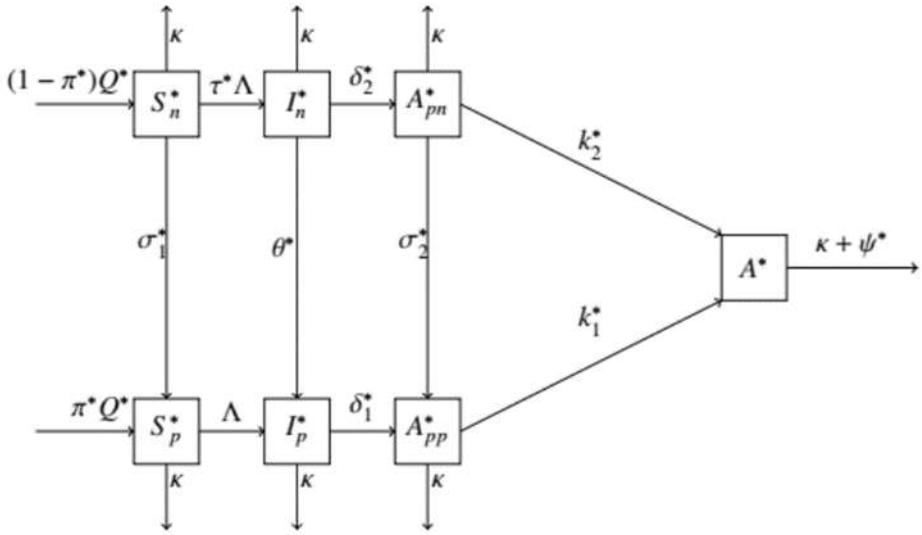

Figure 1. Schematic diagram of the model

therein.

$$
\begin{aligned}
{}^{ABF}D_{0,t}^{\omega,\varrho}S_p^* &= \pi^*Q^* + \sigma_1^*S_n^* - (\Lambda+\kappa)S_p^*,\\
{}^{ABF}D_{0,t}^{\omega,\varrho}S_n^* &= (1-\pi^*)Q^* - (\tau^*\Lambda+\sigma_1^*+\kappa)S_n^*,\\
{}^{ABF}D_{0,t}^{\omega,\varrho}I_p^* &= \Lambda S_p^* + \theta^*I_n^* - (\delta_1^*+\kappa)I_p^*,\\
{}^{ABF}D_{0,t}^{\omega,\varrho}I_n^* &= \tau^*\Lambda S_n^* - (\theta^*+\delta_2^*+\kappa)I_n^*,\\
{}^{ABF}D_{0,t}^{\omega,\varrho}A_{pp}^* &= \delta_1^*I_p^* + \sigma_2^*A_{pn}^* - (\kappa+k_1^*)A_{pp}^*,\\
{}^{ABF}D_{0,t}^{\omega,\varrho}A_{pn}^* &= \delta_2^*I_n^* - (\sigma_2^*+k_2^*+\kappa)A_{pn}^*,\\
{}^{ABF}D_{0,t}^{\omega,\varrho}A^* &= k_1^*A_{pp}^* + k_2^*A_{pn}^* - (\kappa+\psi^*)A^*.
\end{aligned}
\tag{2.2}
$$

with the initial conditions $S_p^*(0) > 0, S_n^*(0) > 0, I_p^*(0) > 0, I_n^*(0) > 0, A_{pp}^*(0) > 0, A_{pn}^*(0) > 0, A^*(0) > 0$, where all the initial values are positive.

2.4. Qualitative analysis of the model

In this section, we establish some results about existence and uniqueness, feasible region, positivity, equilibrium points, basic reproduction number and its sensitivity, and Ulam-Hyers stability analysis [47–51].

2.4.1. Existence and uniqueness of the model

To show the existence and uniqueness of the dynamic system in Equation (2.2), the Banach space can be defined as,

$$f = \mathcal{F} = \mathbb{K}([0,T]\times\mathbb{R}^7,\mathbb{R}),$$

where $\mathcal{F} = \mathbb{K}[0,T]$ and corresponding norm defined by

$$\|f\| = \max_{t\in[0,T]}[|S_p^*| + |S_n^*| + |I_p^*| + |I_n^*| + |A_{pp}^*| + |A_{pn}^*| + |A^*|].$$

To demonstrate the next point in our results, we define the fixed-point theorem.

Theorem 2.1. *A subset of $\mathbb{Z}$ is Ω which is convex and considers that the two operators P_1 and P_2 with*

a. $P_1(m) + P_2(m) \in \Omega,\ \forall m \in \Omega$,

b. P_1 *is a contraction,*

c. P_2 *is continuous and compact.*

The operator equation $P_1 m + P_2 m = m$ has one or more solutions [52, 53].

Now, let us rewrite Equation (2.2) as Atangana-Baleanu fractal-fractional (ABF).

$$\begin{aligned}
{}^{ABF}D^{\omega}_{0,t}S^*_p &= \varrho t^{\varrho-1} f_1(S^*_p, S^*_n, I^*_p, I^*_n, A^*_{pp}, A^*_{pn}, A^*),\\
{}^{ABF}D^{\omega}_{0,t}S^*_n &= \varrho t^{\varrho-1} f_2(S^*_p, S^*_n, I^*_p, I^*_n, A^*_{pp}, A^*_{pn}, A^*),\\
{}^{ABF}D^{\omega}_{0,t}I^*_p &= \varrho t^{\varrho-1} f_3(S^*_p, S^*_n, I^*_p, I^*_n, A^*_{pp}, A^*_{pn}, A^*),\\
{}^{ABF}D^{\omega}_{0,t}I^*_n &= \varrho t^{\varrho-1} f_4(S^*_p, S^*_n, I^*_p, I^*_n, A^*_{pp}, A^*_{pn}, A^*),\\
{}^{ABF}D^{\omega}_{0,t}A^*_{pp} &= \varrho t^{\varrho-1} f_5(S^*_p, S^*_n, I^*_p, I^*_n, A^*_{pp}, A^*_{pn}, A^*),\\
{}^{ABF}D^{\omega}_{0,t}A^*_{pn} &= \varrho t^{\varrho-1} f_6(S^*_p, S^*_n, I^*_p, I^*_n, A^*_{pp}, A^*_{pn}, A^*),\\
{}^{ABF}D^{\omega}_{0,t}A^* &= \varrho t^{\varrho-1} f_7(S^*_p, S^*_n, I^*_p, I^*_n, A^*_{pp}, A^*_{pn}, A^*).
\end{aligned} \tag{2.3}$$

On behalf of Equation (2.3) and for $t \in f$, we can write

$${}^{ABF}D^{\omega} f(t) = \varrho t^{\varrho-1}\mathcal{F}(t, f(t)), t \in [0, T], f(t) = f_0, 0 < \omega \le 1, 0 < \varrho \le 1, \tag{2.4}$$

with solution Gómez and Atangana [18],

$$f(t) = f_0 + \frac{1-\omega}{ABC(\omega)}\varrho t^{\varrho-1}\mathcal{F}(t, f(t)) + \frac{\omega\varrho}{ABC(\omega)\Gamma(\omega)}\int_0^t \tau^{\varrho-1}(t-\tau)^{\omega-1}\mathcal{F}(\tau, f(\tau))d\tau, \tag{2.5}$$

where

$$\begin{aligned}
f(t) &= (S^*_p, S^*_n, I^*_p, I^*_n, A^*_{pp}, A^*_{pn}, A^*)^T,\\
f_0 &= (S^*_{p0}, S^*_{n0}, I^*_{p0}, I^*_{n0}, A^*_{pp0}, A^*_{pn0}, A^*_0)^T,\\
\mathbb{F}(t, f(t)) &= f_i(S^*_p, S^*_n, I^*_p, I^*_n, A^*_{pp}, A^*_{pn}, A^*, t))^T,\ i = 1, 2, 3, ..., 7.
\end{aligned} \tag{2.6}$$

Let $\mathcal{N} = \mathcal{Q}_1 + \mathcal{Q}_2$,

$$\mathcal{Q}_1(f) = f_0 + \frac{1-\omega}{ABC(\omega)}\varrho t^{\varrho-1}[\mathcal{F}(t, f(t))],$$

$$\mathcal{Q}_2(f) = \frac{\omega\varrho}{ABC(\omega)\Gamma(\omega)}\int_0^t \tau^{\varrho-1}(t-\tau)^{\omega-1}\mathcal{F}(\tau, f(\tau))d\tau.$$

We now demonstrate the fixed-point theory-based qualitative analysis of the system [10, 12, 14, 54, 55].

H1: There will be a constant L_1, L_2, such that $|\mathcal{F}(t, f(t))| \le L_1|f| + L_2$.

H2: There exists a constant $L_{\mathcal{F}} > 0$ such that for every $f, \bar{f} \in f$ as $|\mathcal{F}(t, f) - \mathcal{F}(t, \bar{f})| \leq L_{\mathcal{F}}[|f| - \bar{f}]$.

Theorem 2.2. *The dynamic system is defined in Equation* (2.4) *if* $H1$ *and* $H2$ *hold; then, the model in Equation* (2.2) *has the same number of solutions if*

$$\frac{(1-\omega)}{ABC(\omega)} t^{\varrho-1} L_{\mathcal{F}} < 1.$$

Proof. We prove the theorem based on the above two hypotheses in the following steps

Step I: assume that $\bar{f} \in \Omega$ and that $\Omega = f \in f : \|f\| \leq \chi, \chi > 0$ is a convex closed set. Therefore, for operator Q_1, which is defined in Theorem (2.1), we have,

$$\begin{aligned} \|Q_1(f) - Q_1(\bar{f})\| &= \frac{(1-\omega)}{ABC(\omega)} t^{\varrho-1} \max_{t\in[0,\tau]} |\mathcal{F}(t, f(t)) - \mathcal{F}(t, \bar{f}(t))| \\ &\leq \frac{(1-\omega)}{ABC(\omega)} t^{\varrho-1} L_{\mathcal{F}} \|f - \bar{f}\|. \end{aligned} \tag{2.7}$$

Hence, the operator Q_1 is closed and contractive.

Step II: We demonstrate that Q_2 is compact in comparison form. In addition, we demonstrate that Q_2 is bounded and continuous. As $\mathcal{F}$ is continuous, the operator Q_2 is defined in the entire domain for all f in Ω, as follows:

$$\begin{aligned} \|Q_2\| &= \max_{[0,t]} \frac{\omega\varrho}{ABC(\omega)\Gamma(\omega)} \int_0^t \tau^{\varrho-1}(t-\tau)^{\omega-1} \mathcal{F}(\tau, f(\tau)) d\tau \\ &\leq \frac{\omega\varrho}{ABC(\omega)\Gamma(\omega)} \int_0^t \tau^{\varrho-1}(1-\tau)^{n-1} |\mathcal{F}(\tau, f(\tau))| d\tau \\ &\leq \frac{\varrho[L_1|f|] + L_2 J^{\omega+\varrho-1}}{ABC(\omega)\Gamma(\omega)} [D(\omega, \varrho)]. \end{aligned} \tag{2.8}$$

Hence, as seen in Equation (2.8),the operator Q_2 is bounded for equicontinuity, and let $t_1 > t_2 \in [0, T]$. We have

$$\begin{aligned} |Q_2(f(t_2)) - Q_2(f(t_1))| &= |\frac{\omega}{ABC(\omega\varrho)\Gamma(\omega)}| \int_0^{t_2} (t_2-\tau)^{\omega-1} \tau^{\varrho-1} \mathcal{F}(\tau, f(\tau)) d\tau \\ &\leq \frac{\varrho[L_1|f|] + L_2 J^{\omega+\varrho-1}}{ABC(\omega)\Gamma(\omega)} [D(\omega, \varrho)][t_2^{\omega} - t_1^{\omega}]. \end{aligned} \tag{2.9}$$

□

As time goes $t_2 \to t_1$, the right-hand side of the Equation (2.9) approaches zero. Therefore, the operator Q_2 continuous such that $|Q_2(f(t_2)) - Q_2(f(t_1))| \to 0$, as $t_2 \to t_1$.

Hence, we show that the operator Q_2 is bounded and continuous; thus, Q_2 is bounded and uniformly continuous. According to the Arzela-Ascoli theorem, subset $f \in \Omega$ of Q_2 is compact if and only if it is closed, bounded, and equicontinuous. Q_2 is relatively compact and completely continuous. From Equation (2.8) and Equation (2.9), we conclude that the model (2.2) has at least one solution.

2.4.2. Uniqueness of solutions

Theorem 2.3. *With hypothesis* (H_2) *and Equation* (2.5)*, there is a unique solution, so that the dynamical system Equation* (2.2) *also has a unique solution if*

$$\left[\frac{(1-\omega)t^{\varrho-1}L_1}{ABC(\omega)}+\frac{\varrho[L_{\mathcal{F}}T^{\omega+\varrho-1}]D(\omega,\varrho)}{ABC(\omega)\Gamma(\omega)}\right]<1.$$

Proof. Suppose as the operator $\mathcal{N}: f\to f$ by

$$\begin{aligned}\mathcal{N}f(t)=f_0(t)+[\mathcal{F}(t,f(t))-\mathcal{F}_0(t)]\frac{(1-\omega)t^{\varrho-1}}{ABC(\omega)}+\\ \frac{\omega\varrho}{ABC(\omega)\Gamma(\omega)}\int_0^t(t-x)^{\omega-1}t^{\varrho-1}|\mathcal{F}(x,f(x))|dx, t\in[0,\tau].\end{aligned}\tag{2.10}$$

Let $f,\bar{f}\in f$. Then,

$$\begin{aligned}\|\mathcal{N}f-\mathcal{N}\bar{f}\|&\leq\frac{(1-\omega)t^{\varrho-1}}{ABC(\omega)}\max_{t\in[0,\tau]}|\mathcal{F}(t,f(t))-\mathcal{F}(t,\bar{f}(t))|+\\ &\frac{\omega\varrho}{ABC(\omega)\Gamma(\omega)}\max_{t\in[0,\tau]}|\int_0^t(t-\tau)^{\omega-1}t^{\varrho-1}\mathcal{F}(\tau,f(\tau))d\tau-\\ &\int_0^t(t-\tau)t^{\omega-1}\mathcal{F}(\tau,\bar{f}(\tau))d\tau|\\ &\leq\theta\|f-\bar{f}\|,\end{aligned}\tag{2.11}$$

and $\theta=\left[\dfrac{(1-\omega)t^{\varrho-1}L_1}{ABC(\omega)}+\dfrac{\varrho[L_{\mathcal{F}}T^{\omega+\varrho-1}]D(\omega,\varrho)}{ABC(\omega)\Gamma(\omega)}\right]$.

From step II and the operator $\mathcal{N}$ is a contraction. Thus, by the Banach fixed-point theorem, the system (2.5) has a unique solution. Thus, the dynamical system in Equation (2.2) has a unique solution. □

2.4.3. Feasible region

Theorem 2.4. *The set* $\Phi=\{(S_p^*,S_n^*,I_p^*,I_n^*,A_{pp}^*,A_{pn}^*,A^*)\in\mathbb{R}_+^7: N\leq\dfrac{Q^*}{\kappa}\}$*, is non-negative. Additionally each solution lies in* $\mathbb{R}_+^7$.

Proof. Since all parameters in the model (2.2) are non-negative and the second equation is fully parameter and the values $0<\pi^*<1$. Hence, change in the S_n^* is non-negative, based on this values all other variables are non-negative.

$$\begin{aligned}{}^{ABF}D_{0,t}^{\omega,\varrho}S_p^*|_{S_p^*=0}&=\pi^*Q^*+\sigma_1^*S_n^*\geq0,\\ {}^{ABF}D_{0,t}^{\omega,\varrho}S_n^*|_{S_n^*=0}&=(1-\pi^*)Q^*\geq0,\\ {}^{ABF}D_{0,t}^{\omega,\varrho}I_p^*|_{I_p^*=0}&=\Lambda S_p^*+\theta^*I_n^*\geq0,\\ {}^{ABF}D_{0,t}^{\omega,\varrho}I_n^*|_{I_n^*=0}&=\tau^*\Lambda S_n^*\geq0,\\ {}^{ABF}D_{0,t}^{\omega,\varrho}A_{pp}^*|_{A_{pp}^*=0}&=\delta_1^*I_p^*+\sigma_2^*A_{pn}^*\geq0,\\ {}^{ABF}D_{0,t}^{\omega,\varrho}A_{pn}^*|_{A_{pn}^*=0}&=\delta_2^*I_n^*\geq0,\\ {}^{ABF}D_{0,t}^{\omega,\varrho}A^*|_{A^*=0}&=k_1^*A_{pp}^*+k_2^*A_{pn}^*\geq0.\end{aligned}\tag{2.12}$$

From the dynamical system Equation (2.2) and total population $N(t)$, we have

$$\begin{aligned}
&{}^{ABF}D_{0,t}^{\omega,\varrho}N(t)\\
=&{}^{ABF}D_{0,t}^{\omega,\varrho}S_p^* + {}^{ABF}D_{0,t}^{\omega,\varrho}S_n^* + {}^{ABF}D_{0,t}^{\omega,\varrho}I_p^* + {}^{ABF}D_{0,t}^{\omega,\varrho}I_n^* + {}^{ABF}D_{0,t}^{\omega,\varrho}A_{pp}^*\\
&+ {}^{ABF}D_{0,t}^{\omega,\varrho}A_{pn}^* + {}^{ABF}D_{0,t}^{\omega,\varrho}A^* \qquad (2.13)\\
=&Q^* - \kappa S_p^* - \kappa S_n^* - \kappa I_p^* - \kappa I_n^* - \kappa A_{pp}^* - \kappa A_{pn}^* - (\kappa+\psi)A^*\\
=&Q^* - \kappa N - \psi A^* \le Q^* - \kappa N,
\end{aligned}$$

$$ {}^{ABF}D_{0,t}^{\omega,\varrho}N(t) \le Q^* - \kappa N. \qquad (2.14)$$

We can write the fractal-fractional Equations (2.14),

$$ {}^{ABC}D_{0,t}^{\omega}N(t) \le \varrho t^{\varrho-1}(Q^* - \kappa N(t)), \qquad (2.15)$$

By applying the Laplace transform to the linear fractal-fractional Equation (2.15), we obtain:

$$\mathcal{L}\{{}^{ABC}D_t^{\omega}f(t) + \kappa\varrho t^{\varrho-1}N(t)\} \le \mathcal{L}\{\varrho t^{\varrho-1}Q^*\},$$

where $k_1 = \dfrac{-(1-\omega)\kappa}{\beta(\omega)}$,

$$\mathcal{L}\{{}^{ABC}D_t^{\omega}f(t) - \frac{\beta(\omega)}{1-\omega}k_1\varrho t^{\varrho-1}N(t)\} \le \mathcal{L}\{\rho t^{\varrho-1}Q^*\},$$

$$\frac{\beta(\omega)}{1-\omega}\left(\frac{s^{\omega}\hat{f}(s) - s^{\omega-1}f(0)}{s^{\omega}+\dfrac{\omega}{1-\omega}} - k_1\frac{\varrho\Gamma(\varrho)}{s^{\varrho}}\hat{f}(s)\right) = \frac{Q^*\rho\Gamma(\varrho)}{s^{\varrho}},$$

$$\frac{\beta(\omega)}{1-\omega}\left(\frac{s^{\omega}\hat{f}(s) - s^{\omega-1}f(0) - k_1\varrho\Gamma(\varrho)s^{-\varrho}(s^{\omega}+\dfrac{\omega}{1-\omega})\hat{f}(s)}{s^{\omega}+\dfrac{\omega}{1-\omega}}\right) = \frac{Q^*\varrho\Gamma(\varrho)}{s^{\varrho}}\left(s^{\alpha}+\frac{\omega}{1-\omega}\right),$$

$$\left(s^{\omega}\hat{f}(s) - s^{\omega-1}f(0) - k_1\rho\Gamma(\varrho)s^{-\varrho}(s^{\omega}+\frac{\omega}{1-\omega})\hat{f}(s)\right) = \frac{1-\omega}{\beta(\omega)}\frac{Q^*\varrho\Gamma(\varrho)}{s^{\varrho}}\left(s^{\omega}+\frac{\omega}{1-\omega}\right),$$

$$\left(s^{\omega}\hat{f}(s) - k_1\varrho\Gamma(\varrho)s^{-\varrho}(s^{\omega}+\frac{\omega}{1-\omega})\hat{f}(s)\right) = \frac{1-\omega}{\beta(\omega)}\frac{Q^*\varrho\Gamma(\varrho)}{s^{\varrho}}\left(s^{\omega}+\frac{\omega}{1-\omega}\right) + s^{\omega-1}f(0),$$

$$\hat{f}(s)\left(s^{\omega} - k_1\varrho\Gamma(\varrho)s^{-\varrho}(s^{\omega}+\frac{\omega}{1-\omega})\right) = \frac{1-\omega}{\beta(\omega)}\frac{Q^*\rho\Gamma(\varrho)}{s^{\varrho}}\left(s^{\omega}+\frac{\omega}{1-\omega}\right) + s^{\omega-1}f(0),$$

$$\begin{aligned}
&\hat{f}(s)\left((1-k_1\varrho\Gamma(\varrho)s^{-\varrho})s^{\omega} - k_1\varrho\Gamma(\varrho)s^{-\varrho}\frac{\omega}{1-\omega}\right)\\
&\quad= \frac{1-\omega}{\beta(\omega)}\frac{Q^*\varrho\Gamma(\varrho)}{s^{\varrho}}\left(s^{\omega}+\frac{\omega}{1-\omega}\right) + s^{\omega-1}f(0),
\end{aligned}$$

where $K = k_1\rho\Gamma(\varrho)s^{-\varrho}$,

$$\hat{f}(s)\left((1-K)s^{\omega} - K\frac{\omega}{1-\omega}\right) = \frac{1-\omega}{\beta(\omega)}Q^*\frac{K}{k_1}\left(s^{\omega}+\frac{\omega}{1-\omega}\right) + s^{\omega-1}f(0),$$

$$\hat{f}(s)\left((1-\frac{K\omega}{(1-\omega)(1-K)}s^{-\omega}\right) = \frac{1-\omega}{\beta(\omega)(1-K)}Q^*\frac{K}{k_1}\left(1+\frac{\omega}{1-\omega}s^{-\omega}\right) + \frac{1}{(1-K)s}f(0),$$

$$\hat{f}(s) = \left[(1-\frac{K\omega}{(1-\omega)(1-K)}s^{-\omega}\right]^{-1}\left[\frac{1-\omega}{\beta(\omega)(1-K)}Q^*\frac{K}{k_1}\left(1+\frac{\omega}{1-\omega}s^{-\omega}\right) + \frac{1}{(1-K)s}f(0)\right],$$

where $K = k_1\rho\Gamma(\varrho)s^{-\varrho}$, which the Laplace inverse of K is $k_1\varrho t^{\varrho-1}$. Following the work [56,57] and applying the inverse Laplace transform, the solution is given by,

$$\begin{aligned} N(t) =& \frac{Q^*}{\kappa} - \frac{Q^*}{\kappa(1-K)}\frac{d}{dt^\rho}\int_0^t E_{\alpha,\rho}\left(\frac{K\alpha}{(1-K)(1-\alpha)}(t-x)^\alpha dx\right) \\ &+ \frac{1}{1-K}E_{\alpha,\rho}\left(\frac{K\alpha}{(1-K)(1-\alpha)}t^\alpha\right)N(0), \\ N(t) =& \frac{Q^*}{\kappa} - \frac{Q^*}{\kappa(1-k_1\varrho t^{\varrho-1})}\frac{d}{dt^\rho}\int_0^t E_{\alpha,\rho}\left(\frac{k_1\varrho t^{\varrho-1}\alpha}{(1-k_1\varrho t^{\varrho-1})(1-\alpha)}(t-x)^\alpha dx\right) \\ &+ \frac{1}{1-k_1\varrho t^{\varrho-1}}E_{\alpha,\rho}\left(\frac{k_1\varrho t^{\varrho-1}\alpha}{(1-k_1\varrho t^{\varrho-1})(1-\alpha)}t^\alpha\right)N(0), \end{aligned} \tag{2.16}$$

where $E_{\alpha,\rho}(Z) = \sum_{n=1}^{\alpha}\frac{Z^{-n}}{\Gamma(\rho-\alpha n)} + O(|z|^{-1-\alpha}), |z| \to \infty, \frac{\alpha\pi}{2} < |arg(z)| \leq \pi$, it is not difficult to observe that $N(t) \to \frac{Q^*}{\kappa}$ as $t \to \infty$. This leads us to the conclusion that the model is both epidemiologically feasible and well-posed in Φ. □

2.4.4. Equilibrium point of the model and reproduction number

Finding the exact solutions to the system in Equation (2.1) is analytically intractable but we can still gain qualitative knowledge of their dynamics through the stability of their equilibrium points. First, we discuss a special solution to this system. The system has two equilibrium points: disease-free equilibrium (DFE) and endemic equilibrium (EE) points.

$$DFE = \left(s_p^0, s_n^0, i_p^0, i_n^0, a_{pp}^0, a_{pn}^0, a^0\right) = \left(\frac{Q^*(\pi^*\kappa+\sigma_1^*)}{\chi_2}, \frac{(1-\pi^*)Q^*}{\chi_2}, 0, 0, 0, 0, 0\right), \tag{2.17}$$

where $\chi_2 = \sigma_1^* + \kappa, \chi_3 = \delta_1^* + \kappa, \chi_4 = \theta^* + \delta_2^* + \kappa, \chi_5 = \kappa + k_1^*, \chi_6 = \sigma_2^* + k_2^* + \kappa, \chi_7 = \kappa + \psi^*$, and the endemic equilibrium point if all state variables are different from zero, and we obtain,

$$\bar{S}_p^* = \frac{Q^*\pi(\tau\lambda^*+\chi_2)+\sigma_1 Q^*(1-\pi)}{(\lambda^*+\kappa)(\tau^*\lambda^*+\chi_2)},$$

$$\bar{S}_n^* = \frac{(1-\pi)Q^*}{\tau^*\lambda^*+\chi_2}, \bar{I}_p^* = \frac{\Lambda[\pi^*Q^*(\tau^*\Lambda+\kappa)+\sigma_1^*Q^*]}{\chi_3(\Lambda+\kappa)(\tau^*\Lambda+\chi_2)} + \frac{\theta^*\tau^*Q^*\Lambda(1-\pi^*)}{\chi_3\chi_4(\tau^*\Lambda+\chi_2)},$$

$$\bar{I_n}^* = \frac{\tau^*\Lambda(1-\pi^*)Q^*}{(\tau^*\Lambda^*+\chi_2)\chi_4}, \bar{A}_{pn}^* = \frac{\delta_2^*\tau^*\Lambda Q^*(1-\pi^*)}{(\tau^*\Lambda+\chi_2)\chi_4\chi_6},$$

$$\bar{A}_{pp} = \frac{\delta_1^*\Lambda[\pi^*Q^*(\tau^*\Lambda+\kappa)+\sigma_1^*Q^*]}{\chi_3\chi_5(\Lambda+\kappa)(\tau^*\Lambda+\chi_2)} + \frac{\delta_1^*\theta^*\tau^*\Lambda(1-\pi^*)Q^*}{(\tau^*\Lambda^*+\chi_2)\chi_3\chi_4\chi_5}, \bar{A}^* = \frac{k_1^*a_{pp}^* + k_2^*a_{pn}^*}{\chi_7},$$

where the force of infection at the equilibrium point is

$$\begin{aligned} \Lambda^* =& \frac{\Lambda^*[\pi^*Q^*(\tau^*\Lambda^*+\kappa)+\sigma_1^*Q^*]}{\chi_3(\Lambda^*+\kappa)(\tau^*\Lambda^*+\chi_2)} + \frac{\theta^*\tau^*Q^*\Lambda^*(1-\pi^*)}{\chi_3\chi_4(\tau^*\Lambda^*+\chi_2)} \\ &+ \frac{\tau^*\Lambda^*(1-\pi^*)Q^*}{(\tau^*\Lambda^*+\chi_2)\chi_4} + \frac{\delta_2^*\tau^*\Lambda^*Q^*(1-\pi^*)}{(\tau^*\Lambda^*+\chi_2)\chi_4\chi_6} \\ &+ \frac{\delta_1^*\Lambda^*[\pi^*Q^*(\tau^*\Lambda^*+\kappa)+\sigma_1^*Q^*]}{\chi_3\chi_5(\Lambda^*+\kappa)(\tau^*\Lambda^*+\chi_2)} \\ &+ \frac{\delta_1^*\theta^*\tau^*\Lambda^*(1-\pi^*)Q^*}{(\tau^*\Lambda^*+\chi_2)\chi_3\chi_4\chi_5} \geq 0. \end{aligned}$$

After algebraic simplification and rearrangement, we obtain $\Lambda^* = 0$ and the following:

$$\frac{[\pi^* Q^*(\tau^*\Lambda^* + \kappa) + \sigma_1^* Q^*]}{\chi_3(\Lambda^* + \kappa)(\tau^*\Lambda^* + \chi_2)} + \frac{\theta^*\tau^* Q^*(1-\pi^*)}{\chi_3\chi_4(\tau^*\Lambda^* + \chi_2)} + \frac{\tau^*(1-\pi^*)Q^*}{(\tau^*\Lambda^* + \chi_2)\chi_4} + \frac{\delta_2^*\tau^* Q^*(1-\pi^*)}{(\tau^*\Lambda^* + \chi_2)\chi_4\chi_6} + \frac{\delta_1^*[\pi^* Q^*(\tau^*\Lambda^* + \kappa) + \sigma_1^* Q^*]}{\chi_3\chi_5(\Lambda^* + \kappa)(\tau^*\Lambda^* + \chi_2)} + \frac{\delta_1^*\theta^*\tau^*(1-\pi^*)Q^*}{(\tau^*\Lambda^* + \chi_2)\chi_3\chi_4\chi_5} \geq 0,$$

$$a_1 = \chi_4\chi_6\pi^*\kappa\tau^*(\chi_5 + \delta_1^*) + \chi_5\kappa\tau^*(1-\pi^*)(\chi_6\theta^* + \chi_6\chi_3 + \chi_3\delta_2^*),$$
$$a_0 = \chi_4\chi_6\kappa(\kappa\pi^* + \sigma_1^*)(\chi_5\pi^* + \delta_1^*) + \chi_5\kappa^2\tau^*(1-\pi^*)(\chi_6\theta^* + \chi_6\chi_3 + \chi_3\delta_2^*),$$

$$a_1\Lambda^* + a_0 \geq 0. \tag{2.18}$$

Therefore, an endemic equilibrium point exists at a value greater than or equal to zero in this linear equation. Using the next-generation matrix methods Driessche and Watmough [51], we calculated the reproduction number as follows:

$$R_0 = \frac{\beta(\delta_1\chi_4\chi_6 + \chi_4\chi_5\chi_6)S_p^0 + (\delta_1\chi_6\tau^*\theta + \delta_2\chi_3\chi_5\tau^* + \chi_3\chi_5\chi_6\tau^* + \chi_5\chi_6\tau\theta)S_n^0}{\chi_3\chi_4\chi_5\chi_6} \tag{2.19}$$

and if $R_0 < 1$, the disease can be eliminated, and if $R_0 > 1$, the disease persists in the population.

2.4.5. Stability of disease free equilibrium

Theorem 2.5. *If R_0 is less than 1, the model has a disease-free equilibrium point E_0 that is asymptotically stable as long as the proportions of each susceptible group to the total population at any time t do not exceed their corresponding proportions at DFE. In other words, DFE is asymptotically stable if the following conditions hold.*

$$S_p^* \leq \frac{Q^*(\pi^*\kappa + \sigma_1^*)}{\chi_1}, S_n^* \leq \frac{(1-\pi^*)Q^*}{\chi_2}. \tag{2.20}$$

Proof. Let the set $X = (S_p^*, S_n^*)$ and $Y = (I_p^*, I_n^*, A_{pp}^*, A_{pn}^*, A^*)$ the working-class mathematical model of HIV/AIDS infection (2.2) can be rewritten as;

$$\begin{aligned} \frac{dX}{dt} &= F(X,Y), \\ \frac{dY}{dt} &= G(X,Y), \end{aligned} \tag{2.21}$$

where

$$F = \begin{cases} \pi^* Q^* + \sigma_1^* S_n^* - (\Lambda + \kappa)S_p^*, \\ (1-\pi^*)Q^* - (\tau^*\Lambda + \sigma_1^* + \kappa)S_n^*, \end{cases}$$

$$and, G = \begin{cases} \Lambda S_p^* + \theta^* I_n^* - (\delta_1^* + \kappa)I_p^*, \\ \tau^*\Lambda S_n^* - (\theta^* + \delta_2^* + \kappa)I_n^*, \\ \delta_1^* I_p^* + \sigma_2^* A_{pn}^* - (\kappa + k_1^*)A_{pp}^*, \\ \delta_2^* I_n^* - (\sigma_2^* + k_2^* + \kappa)A_{pn}^*, \\ k_1^* A_{pp}^* + k_2^* A_{pn}^* - (\kappa + \psi^*)A^*. \end{cases} \tag{2.22}$$

Then, disease-free equilibrium points are stable if the following two conditions by Castillo-Chavez [58] are hold.

C_1**:** For $\frac{dX}{dt}|_{Z=0}, X^*$ is asymptotically stable,

C_2**:** $G(X,Y) = LY - \hat{G}(X,Y), \hat{G}(X,Y) \geq 0$ for $(X,Y) \in \mathbb{R}^7_+$,

where $L = D_{Y=0}G(X^*,0)$ is the jacobian of $G(X,Y)$ with respect to Y evaluated at disease free equilibrium. The reduced system at disease free equilibrium point,

$$\frac{dX}{dt}|_{Y=0} = \begin{cases} \pi^* Q^* + \sigma_1^* S_n^* - \kappa S_p^*, \\ (1-\pi^*)Q^* - (\sigma_1^* + \kappa)S_n^*. \end{cases}$$

The disease-free equilibrium point is equal to X^* is globally asymptotically stable point of the reduced system, here all solutions of the reduced system is equal with the disease free equilibrium point as time goes to infinity

Moreover $G(X,Y) = LY - \hat{G}(X,Y)$,where $L = D_{Y=0}G(X^*,0)$

$$L = \begin{bmatrix} \frac{\beta^* S_p^{*0}}{N} - \chi_3 & \frac{\beta^* S_p^{*0}}{N} + \theta^* & \frac{\beta^* S_p^{*0}}{N} & \frac{\beta^* S_p^{*0}}{N} & 0 \\ \frac{\tau^* \beta^* S_n^{*0}}{N} & \frac{\tau^* \beta^* S_n^{*0}}{N} - \chi_4 & \frac{\tau^* \beta^* S_n^{*0}}{N} & \frac{\tau^* \beta^* S_n^{*0}}{N} & 0 \\ \delta_1^* & 0 & -\chi_5 & 0 & 0 \\ 0 & \delta_2^* & 0 & -\chi_6 & 0 \\ 0 & 0 & k_1^* & k_2^* & -\chi_7 \end{bmatrix},$$

$$LY = \begin{bmatrix} \frac{\beta S_p^{*0}}{N} - \chi_3 & \frac{\beta S_p^{*0}}{N} + \theta & \frac{\beta S_p^{*0}}{N} & \frac{\beta S_p^{*0}}{N} & 0 \\ \frac{\tau \beta S_n^{*0}}{N} & \frac{\tau \beta S_n^{*0}}{N} - \chi_4 & \frac{\tau \beta S_n^{*0}}{N} & \frac{\tau \beta S_n^{*0}}{N} & 0 \\ \delta_1^* & 0 & -\chi_5 & 0 & 0 \\ 0 & \delta_2^* & 0 & -\chi_6 & 0 \\ 0 & 0 & k_1 & k_2 & -\chi_7 \end{bmatrix} \begin{bmatrix} I_p^* \\ I_n^* \\ A_{pp}^* \\ A_{pn}^* \\ A^* \end{bmatrix},$$

$$LY = \begin{bmatrix} (\frac{\beta S_p^{*0}}{N} - \chi_3)I_p^* + (\frac{\beta S_p^{*0}}{N} + \theta)I_n^* + \frac{\beta S_p^{*0}}{N} A_{pp}^* + \frac{\beta S_p^{*0}}{N} A_{pn}^* \\ \frac{\tau^* \beta S_n^{*0}}{N} I_p^* + (\frac{\tau^* \beta S_n^{*0}}{N} - \chi_4)I_n^* + \beta\tau S_n^* A_{pp}^* + \beta\tau S_n^* A_{pn}^* \\ \delta_1 I_p^* - \chi_5 A_{pp}^* \\ \delta_2 I_n^* - \chi_6 A_{pn}^* \\ k_1 A_{pp}^* k_2 A_{pn}^* - \chi_7 A^* \end{bmatrix},$$

$$\hat{G}(X,Y) = LY - G(X,Y) = \Lambda \begin{bmatrix} (S_p^{*0} - S_p^*) \\ \tau^*(S_n^{*0} - S_n^*) \\ 0 \\ 0 \\ 0 \end{bmatrix} \geq 0,$$

where $\Lambda = \beta^*(\frac{I_p^* + I_n^* + A_{pp}^* + A_{pn}}{N})$.

Now, we have $S_p^{*0} - S_p^* \geq 0$ and $S_n^{*0} - S_n^* \geq 0$, which implies that that condition C_2 satisfied if and only if $S_p^* \leq S_p^{*0}$ and $S_n^* \leq S_n^{*0}$

$$S_p^* \leq \frac{Q^*(\pi^*\kappa + \sigma_1^*)}{\chi_1}, S_n^* \leq \frac{(1-\pi^*)Q^*}{\chi_2},$$

this completes the proof. □

2.4.6. Sensitivity analysis

Sensitivity analysis of reproduction numbers gives the information which parameters are most important to control the transmission and spread of the disease. From the reproduction number stated in Equation (2.19) its sensitivity index to the parameters ρ if ρ is a parameter in the R_0 is given by $S_\rho = \frac{\partial R_0}{\partial \rho}\frac{\rho}{R_0}$. The result is given in the Table 2. The reproduction number increases if the sensitivity index is positive, and decreases if negative. When a sign is positive, it indicates that the reproduction number rises as the parameter rises, and when it is negative, the converse is true. As we can see from Figure 2, $\beta^*, \theta^*, k_1^*, k_2^*, \tau^*, \delta_1^*, \delta_2^*$ have positive effects on reproduction number, but $\sigma_1^*, \sigma_2^*, \pi^*$ have negative effects as illustrated in Figure 2.

Parameter	Sensitivity indices	Parameters	Sensitivity indices
θ^*	-0.042	k_2^*	0
σ_1^*	-0.0423	τ^*	0.2696
π^*	0.1321	δ_1^*	0.3527
k_1^*	0.6108	δ_2^*	0.1604
k_2^*	0.1494	σ_2^*	-0.0623

Table 2. Sensitivity indices of the parameters

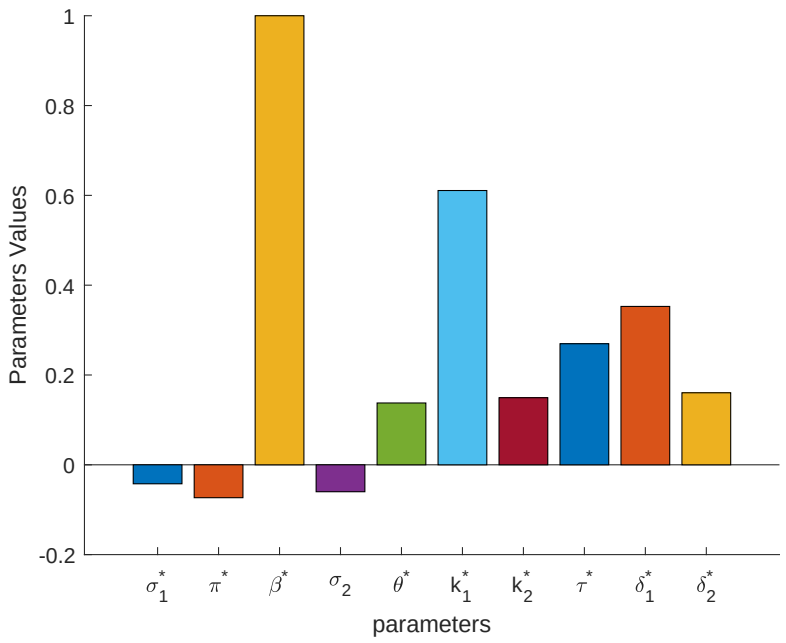

Figure 2. Sensitivity index of parameters

2.4.7. Ulam-Hyers stability

In this section, we determine the stability of the proposed mathematical model of the fractal-fractional-order Equation (2.2). To do this, let us take a small perturbation $\Xi(t) \in C[0,T]$ and only satisfy $\Xi(0) = 0$ as follows:

$$\Xi(t) \leq \epsilon \quad \text{for} \quad \epsilon > 0;$$

$$^{ABC}D_t^{\omega,\varrho} f(t) = \mathcal{F}(t, f(t)) + \Xi(t).$$

The solution of the perturbed dynamical system can be

$$^{ABC}D_t^{\omega,\varrho} f(t) = \mathcal{F}(t, f(t)) + \Xi(t), \quad f(0) = f_0, \tag{2.23}$$

and satisfies the following equation [47, 48, 59].

$$\begin{aligned} f(t) - \Bigg(f_0(t) + [\mathcal{F}(t, f(t)) - \Xi_0(t)] \frac{(1-\omega)t^{\varrho-1}}{ABC(\omega)} \\ + \frac{\omega\varrho}{ABC(\omega)\Gamma(\omega)} \int_0^t (t-x)^{\omega-1} x^{\varrho-1} \mathcal{F}(x, f(x))\, dx \Bigg) \\ \leq \frac{\Gamma(\omega)t^{\varrho-1} + \varrho T^{\omega+\varrho-1}}{ABC(\omega)\Gamma(\omega)} D(\omega,\varrho)\epsilon = \omega_{\omega\varrho}\epsilon. \end{aligned} \tag{2.24}$$

Theorem 2.6. *Under Hypothesis H2, solutions to Equation* (2.5) *are Ulam-Hyers stable if* $\left[\frac{(1-\omega)t^{\varrho-1}L_1}{ABC(\omega)} + \frac{\varrho[L_{\mathcal{F}} T^{\omega+\varrho-1}] D(\omega,\varrho)}{ABC(\omega)\Gamma(\omega)} \right] < 1.$

Proof. Assume that a unique solution is $f \in f$ and that $\bar{f} \in f$ is any solution of Equation (2.5)); then,

$$\begin{aligned}
|f(t) - \bar{f}(t)| =& |f(t) - \left(f_0(t) + [\mathcal{F}(t, f(t)) - f_0(t)] \frac{1-\omega}{ABC(\omega)} t^{\varrho-1} \right) \\
& - \left(\frac{\omega\varrho}{ABC(\omega)\Gamma(\omega)} \times \int_0^t x^{\varrho-1}(t-x)^{\omega-1} \mathcal{F}(x, \bar{f}(x)) dx \right) | \\
\leq & |f(t) - \left(f_0(t) + [\mathcal{F}(t, f(t)) - f_0(t)] \frac{1-\omega}{ABC(\omega)} t^{\varrho-1} \right) \\
& - \left(\frac{\omega\varrho}{ABC(\omega)\Gamma(\omega)} \times \int_0^t x^{\varrho-1}(t-x)^{\omega-1} \mathcal{F}(x, f(x)) dx \right) | \\
& - | \left(f_0(t) + [\mathcal{F}(t, \bar{f}(t)) - f_0(t)] \frac{1-\omega}{ABC(\omega)} t^{\varrho-1} \right) | \\
& - | \left(\frac{\omega\varrho}{ABC(\omega)\Gamma(\omega)} \times \int_0^t x^{\varrho-1}(t-x)^{\omega-1} \mathcal{F}(x, \bar{f}(x)) dx \right) | \\
\leq & \omega_{\omega\varrho} + \frac{(1-\omega)L_{\mathcal{F}}}{ABC(\omega)} t^{\varrho-1} \|f - \bar{f}\| + \frac{\varrho T^{\omega+\varrho-1} L_{\mathcal{F}}}{ABC(\omega)\Gamma(\omega)} D(\omega, \varrho) \|f - \bar{f}\| \\
\leq & \omega_{\omega\varrho} + \theta \|f - \bar{f}\|.
\end{aligned} \tag{2.25}$$

From Equation (2.25) we can express as

$$\|f - \bar{f}\| \leq \frac{\omega_{\omega\varrho}}{1-\theta} \|f - \bar{f}\|. \tag{2.26}$$

From Equation (2.26), we conclude that the solution of Equation (2.5) is Ulam-Hyres stable and generalized Ulam-Hyers stable by using $\mathcal{F}_f(\epsilon) = \omega_{\omega\varrho}\epsilon,\ \mathcal{F}_f(0) = 0$, which shows that the proposed fractal-fractional model is Ulam-Hyers stable and generalized Ulam-Hyers stability. □

3. Numerical solutions

3.1. Parameter estimation

We calibrate the model using WHO and UNAIDS data from Ethiopia (2001–2023). The least-square method was used to estimate the values of the parameters. As we show in Figure 3, the values of the estimated parameters are stated in Table 1. We use MATLAB 2019b to fit the model by using least square methods with minimum error 0.0011. Absolute errors per iteration for infected productive and non-productive populations are shown in Figures (4)-(5) (box plots).

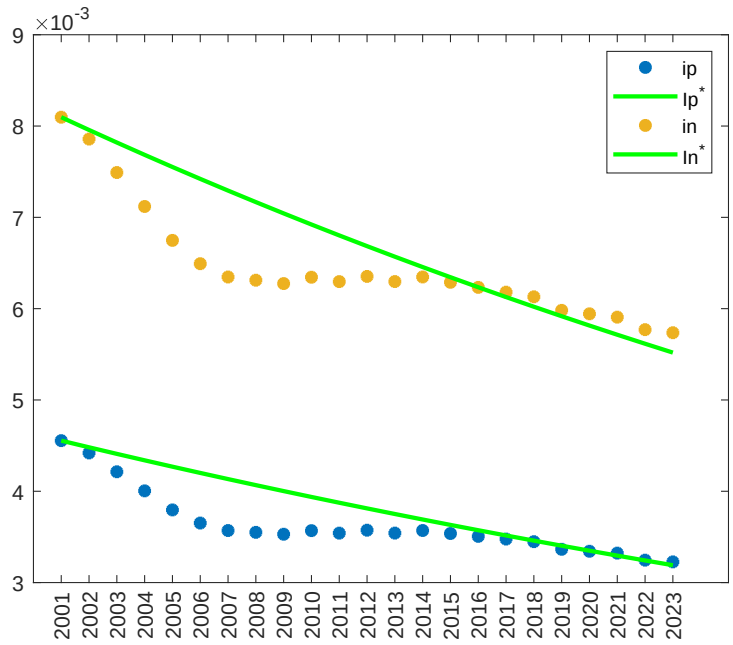

Figure 3. Real data fitted to the nondimensional model to estimate the parameters in Table 1

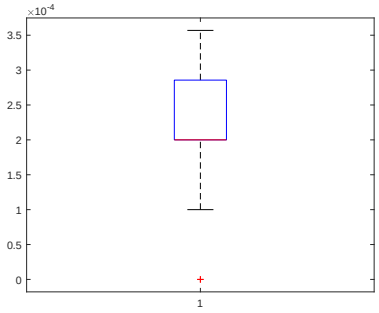

Figure 4. Error iteration of I_P

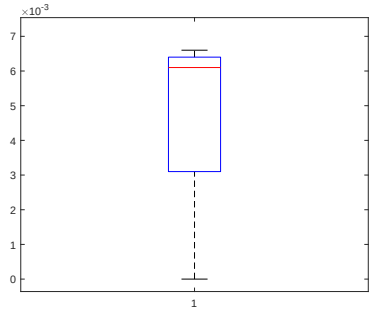

Figure 5. Error iteration of I_n

3.2. Numerical scheme for simulations of the fractional-order model

Numerical techniques are acknowledged as effective mathematical tools for solving nonlinear fractional-order differential equations with local and nonlocal operators. A novel numerical approach for the nonlinear fractional derivatives of ABC, derived in [41, 60],is used to solve the constructed fractional-order model. We adopted this method because it was suitable for our models, and from the constructed fractional-order Equation (2.1), we can write the kernel function of fractional models as Atan-

gana [12].

$$\begin{aligned}
{}_0^{ABC}D_t^{\omega} S_p^*(t) &= M_1(t, S_p^*),\\
{}_0^{ABC}D_t^{\omega} S_n^*(t) &= M_2(t, S_n^*),\\
{}_0^{ABC}D_t^{\omega} I_p^*(t) &= M_3(t, I_p^*),\\
{}_0^{ABC}D_t^{\omega} I_n^*(t) &= M_4(t, I_n^*),\\
{}_0^{ABC}D_t^{\omega} A_{pp}^*(t) &= M_5(t, A_{pp}^*),\\
{}_0^{ABC}D_t^{\omega} A_{pn}^*(t) &= M_6(t, A_{pn}^*),\\
{}_0^{ABC}D_t^{\omega} A^*(t) &= M_7(t, A^*).
\end{aligned} \tag{3.1}$$

The following equation is obtained from Equation (3.1) by means of the fractional-order ABC-integral operator:

$$\begin{aligned}
&S_p^*(t) - S_p^*(0)\\
=&\frac{1-\omega}{ABC(\omega)} M_1(t, S_p^*) + \frac{\omega}{ABC(\omega)\Gamma(\omega)} \int_0^t (t - S_p^*)^{\omega-1} M_1(\tau, S_p^*) d\tau,\\
&S_n^*(t) - S_n^*(0)\\
=&\frac{1-\omega}{ABC(\omega)} M_2(t, S_n^*) + \frac{\omega}{ABC(\omega)\Gamma(\omega)} \int_0^t (t - S_n^*)^{\omega-1} M_2(\tau, S_n^*) d\tau,\\
&I_p^*(t) - I_p^*(0)\\
=&\frac{1-\omega}{ABC(\omega)} M_3(t, I_p^*) + \frac{\omega}{ABC(\omega)\Gamma(\omega)} \int_0^t (t - I_p^*)^{\omega-1} M_3(\tau, I_p^*) d\tau,\\
&I_n^*(t) - I_n^*(0)\\
&= \frac{1-\omega}{ABC(\omega)} M_4(t, I_n^*) + \frac{\omega}{ABC(\omega)\Gamma(\omega)} \int_0^t (t - I_n^*)^{\omega-1} M_4(\tau, I_n^*) d\tau,\\
&A_{pp}^*(t) - A_{pp}^*(0)\\
=&\frac{1-\omega}{ABC(\omega)} M_5(t, A_{pp}^*) + \frac{\omega}{ABC(\omega)\Gamma(\omega)} \int_0^t (t - A_{pp}^*)^{\omega-1} M_5(\tau, A_{pp}^*) d\tau,\\
&A_{pn}^*(t) - A_{pn}^*(0)\\
=&\frac{1-\omega}{ABC(\omega)} M_6(t, A_{pn}^*) + \frac{\omega}{ABC(\omega)\Gamma(\omega)} \int_0^t (t - A_{pn}^*)^{\omega-1} M_6(\tau, A_{pn}^*) d\tau,\\
&A^*(t) - A^*(0)\\
&= \frac{1-\omega}{ABC(\omega)} M_7(t, A^*) + \frac{\omega}{ABC(\omega)\Gamma(\omega)} \int_0^t (t - A^*)^{\omega-1} M_7(\tau, A^*) d\tau.
\end{aligned} \tag{3.2}$$

The suggested interval $[0, t]$ can be divided into subintervals using point t_{n+1}, where $n = 0, 1, \cdots$. We can write Equation (3.2) as:

$$S_p^*(t_{n+1}) - S_p^*(0) = \frac{1-\omega}{ABC(\omega)} M_1(t, S_p^*) + \frac{\omega}{ABC(\omega)\Gamma(\omega)} \int_0^t (t - S_p^*)^{\omega-1} M_1(\tau, S_p^*) d\tau, \tag{3.3}$$

Similarly, we can write for all Equation (3.2) in the same manner. Using the Lagrange interpolation technique, we obtain:

$$
\begin{aligned}
S_p^*(t_{n+1}) =& S_p^*(0) + \frac{1-\omega}{ABC(\omega)} M_1(t_{k^*}, S_p^*) \\
&+ \frac{\omega}{ABC(\omega)} \sum_{k^*=0}^{n} \left[\frac{h^\omega M_1(t_{k^*}, S_p^*)}{\Gamma(\omega+2)} a_1 - \frac{h^\kappa M_1(t_{k^*-1}, S_p^*)}{\Gamma(\kappa+2)} a_2 \right], \\
S_n^*(t_{n+1}) =& S_n^*(0) + \frac{1-\omega}{ABC(\omega)} M_2(t_{k^*}, S_n^*) \\
&+ \frac{\omega}{ABC(\omega)} \sum_{k^*=0}^{n} \left[\frac{h^\omega M_2(t_{k^*}, S_n^*)}{\Gamma(\omega+2)} a_1 - \frac{h^\kappa M_2(t_{k^*-1}, S_n^*)}{\Gamma(\kappa+2)} a_2 \right], \\
I_p^*(t_{n+1}) =& I_p^*(0) + \frac{1-\omega}{ABC(\omega)} M_2(t_{k^*}, I_p^*) \\
&+ \frac{\omega}{ABC(\omega)} \sum_{k^*=0}^{n} \left[\frac{h^\omega M_3(t_{k^*}, I_p^*)}{\Gamma(\omega+2)} a_1 - \frac{h^\kappa M_3(t_{k^*-1}, I_p^*)}{\Gamma(\kappa+2)} a_2 \right], \\
I_n^*(t_{n+1})| =& I_n^*(0) + \frac{1-\omega}{ABC(\omega)} M_4(t_{k^*}, I_n^*) \\
&+ \frac{\omega}{ABC(\omega)} \sum_{k^*=0}^{n} \left[\frac{h^\omega M_4(t_{k^*}, I_n^*)}{\Gamma(\omega+2)} a_1 - \frac{h^\kappa M_4(t_{k^*-1}, I_n^*)}{\Gamma(\kappa+2)} a_2 \right], \\
A_{pp}^*(t_{n+1}) =& A_{pp}^*(0) + \frac{1-\omega}{ABC(\omega)} M_5(t_{k^*}, A_{pp}^*) \\
&+ \frac{\omega}{ABC(\omega)} \sum_{k^*=0}^{n} \left[\frac{h^\omega M_5(t_{k^*}, A_{pp}^*)}{\Gamma(\omega+2)} a_1 - \frac{h^\kappa M_5(t_{k^*-1}, A_{pp}^*)}{\Gamma(\kappa+2)} a_2 \right], \\
A_{pn}^*(t_{n+1}) =& A_{pn}^*(0) + \frac{1-\omega}{ABC(\omega)} M_6(t_{k^*}, A_{pn}^*) \\
&+ \frac{\omega}{ABC(\omega)} \sum_{k^*=0}^{n} \left[\frac{h^\omega M_6(t_{k^*}, A_{pn}^*)}{\Gamma(\omega+2)} a_1 - \frac{h^\kappa M_6(t_{k^*-1}, A_{pn}^*)}{\Gamma(\kappa+2)} a_2 \right], \\
A^*(t_{n+1}) =& A^*(0) + \frac{1-\omega}{ABC(\omega)} M_7(t_{k^*}, A^*) \\
&+ \frac{\omega}{ABC(\omega)} \sum_{k^*=0}^{n} \left[\frac{h^\omega M_7(t_{k^*}, A^*)}{\Gamma(\omega+2)} a_2 - \frac{h^\kappa M_7(t_{k^*-1}, A^*)}{\Gamma(\kappa+2)} a_2 \right],
\end{aligned}
\tag{3.4}
$$

where

$$
\begin{aligned}
a_1 &= (n+1-k^*)^\kappa (n-k^*+2+\kappa) - (n-k^*)^\kappa (n-k^*+2+2\kappa), \\
a_2 &= (n+1-k^*)^\kappa - (n-k^*)^\kappa (n+1-k^*+\kappa).
\end{aligned}
$$

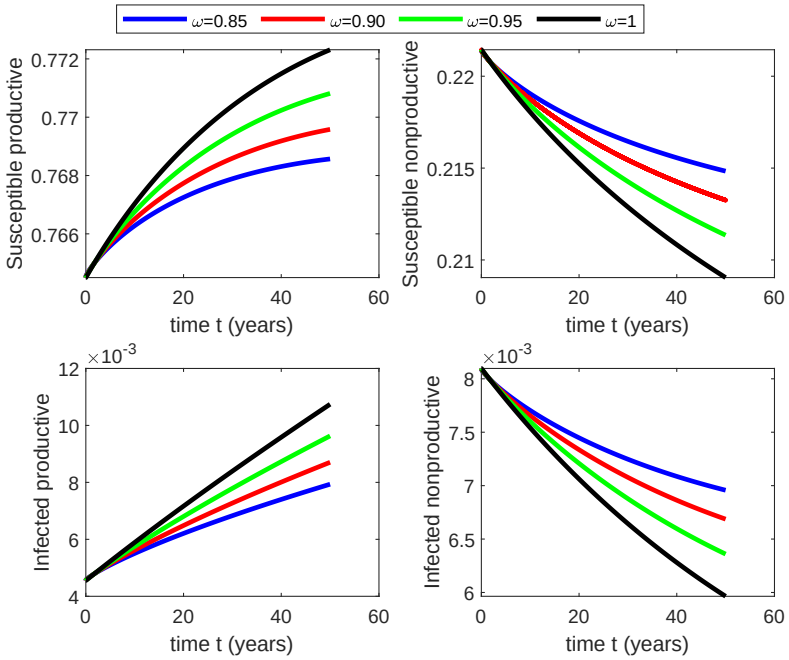

Figure 6. Solutions of the fractional model for different values of fractional order ω

The solutions of the fractional-order model varies depending on the value of ω. If $\omega = 1$, the model restores the integral-order model property. As shown in Figure 6, as the derivative order decreases, the susceptible productive population graph becomes sigmoid and the reality of the model increases. However, susceptible nonproductive populations decreased rapidly, which is relatively unrealistic; infected productive and infected nonproductive populations followed the same pattern. This indicates that the fractional-order derivative model with the Atangana-Baleanu-Caputo operator is better representation of HIV/AIDS infections in the working-class.

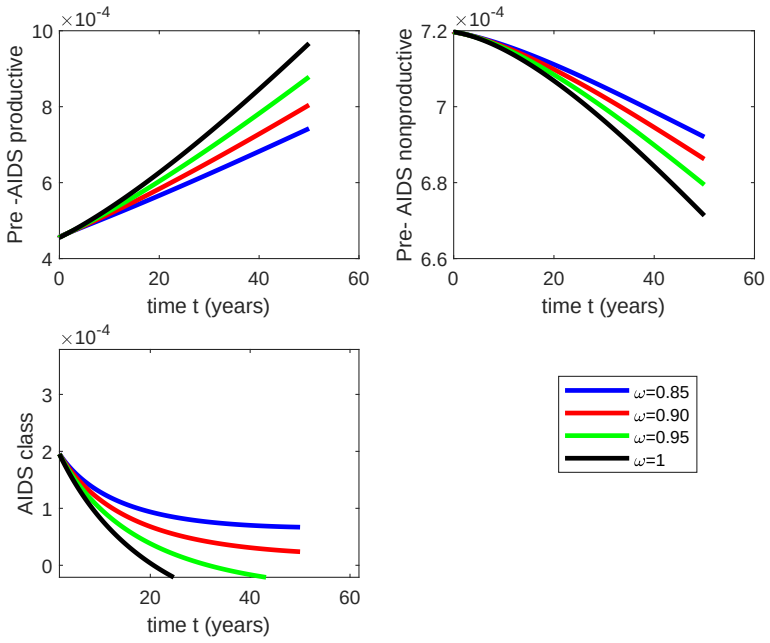

Figure 7. Solution of the fractional model for different values of fractional order ω

The solution of the fractional-order model varies depending on the value of ω; if $\omega = 1$, the model rehabilitates the integral-order model. As shown in Figure 7, as the derivative order decreases, the pre-AIDS productive population decreases, and the pre-AIDS nonproductive population increases rapidly, which is relatively unrealistic. The AIDS class population immediately approaches zero, but the fractional-order model approaches slowly, as we compare it with real data. Hence, the fractional order is a better representation of the real problem of the HIV/AIDS model. This indicates that the fractional-order model is suitable for representing the HIV/AIDS dynamic system.

3.3. Numerical scheme for Atangana-Baleanu-Caputo fractal-fractional model derivative

In this section, we consider the Atangana-Baleanu-Caputo fractal-fractional derivative denoted as (ABF). The model in Equation (2.2), can be expressed as follows:

$$\begin{aligned}
{}^{ABF}D^{\omega}_{0,t}S^*_p &= \varrho t^{\varrho-1} f_1(S^*_p, S^*_n, I^*_p, I^*_n, A^*_{pp}, A^*_{pn}, A^*),\\
{}^{ABF}D^{\omega}_{0,t}S^*_n &= \varrho t^{\varrho-1} f_2(S^*_p, S^*_n, I^*_p, I^*_n, A^*_{pp}, A^*_{pn}, A^*),\\
{}^{ABF}D^{\omega}_{0,t}I^*_p &= \varrho t^{\varrho-1} f_3(S^*_p, S^*_n, I^*_p, I^*_n, A^*_{pp}, A^*_{pn}, A^*),\\
{}^{ABF}D^{\omega}_{0,t}I^*_n &= \varrho t^{\varrho-1} f_4(S^*_p, S^*_n, I^*_p, I^*_n, A^*_{pp}, A^*_{pn}, A^*),\\
{}^{ABF}D^{\omega}_{0,t}A^*_{pp} &= \varrho t^{\varrho-1} f_5(S^*_p, S^*_n, I^*_p, I^*_n, A^*_{pp}, A^*_{pn}, A^*),\\
{}^{ABF}D^{\omega}_{0,t}A^*_{pn} &= \varrho t^{\varrho-1} f_6(S^*_p, S^*_n, I^*_p, I^*_n, A^*_{pp}, A^*_{pn}, A^*),\\
{}^{ABF}D^{\omega}_{0,t}A^* &= \varrho t^{\varrho-1} f_7(S^*_p, S^*_n, I^*_p, I^*_n, A^*_{pp}, A^*_{pn}, A^*),
\end{aligned} \tag{3.5}$$

by applying the Atangana-Baleanu integral formula, we have,

$$
\begin{aligned}
&S_p^*(t)\\
=&S_p^*(0)+\frac{\varrho t^{\varrho-1}(1-\omega)}{ABC(\omega)}f_1(t,\Phi)+\frac{\omega\varrho}{ABC(\omega)\Gamma(\omega)}\int_0^t\tau^{\varrho-1}(t-\tau)^{\omega-1}f_1(\tau,\Phi)d\tau,\\
&S_n^*(t)\\
=&S_n^*(0)+\frac{\varrho t^{\varrho-1}(1-\omega)}{ABC(\omega)}f_2(t,\Phi)+\frac{\omega\varrho}{ABC(\omega)\Gamma(\omega)}\int_0^t\tau^{\varrho-1}(t-\tau)^{\omega-1}f_2(\tau,\Phi)d\tau,\\
&I_p^*(t)\\
=&I_p^*(0)+\frac{\varrho t^{\varrho-1}(1-\omega)}{ABC(\omega)}f_3(t,\Phi)+\frac{\omega\varrho}{ABC(\omega)\Gamma(\omega)}\int_0^t\tau^{\varrho-1}(t-\tau)^{\omega-1}f_3(\tau,\Phi)d\tau,\\
&I_n^*(t)\\
=&I_n^*(0)+\frac{\varrho t^{\varrho-1}(1-\omega)}{ABC(\omega)}f_4(t,\Phi)+\frac{\omega\varrho}{ABC(\omega)\Gamma(\omega)}\int_0^t\tau^{\varrho-1}(t-\tau)^{\omega-1}f_4(\tau,\Phi)d\tau,\\
&A_{pp}^*(t)\\
=&A_{pp}^*(0)+\frac{\varrho t^{\varrho-1}(1-\omega)}{ABC(\omega)}f_5(t,\Phi)+\frac{\omega\varrho}{ABC(\omega)\Gamma(\omega)}\int_0^t\tau^{\varrho-1}(t-\tau)^{\omega-1}f_5(\tau,\Phi)d\tau,\\
&A_{pn}^*(t)\\
=&A_{pn}^*(0)+\frac{\varrho t^{\varrho-1}(1-\omega)}{ABC(\omega)}f_6(t,\Phi)+\frac{\omega\varrho}{ABC(\omega)\Gamma(\omega)}\int_0^t\tau^{\varrho-1}(t-\tau)^{\omega-1}f_6(\tau,\Phi)d\tau,\\
&A^*(t)\\
=&A^*(0)+\frac{\varrho t^{\varrho-1}(1-\omega)}{ABC(\omega)}f_7(t,\Phi)+\frac{\omega\varrho}{ABC(\omega)\Gamma(\omega)}\int_0^t\tau^{\varrho-1}(t-\tau)^{\omega-1}f_7(\tau,\Phi)d\tau.
\end{aligned}
\tag{3.6}
$$

If $\Phi=(S_p^*,S_n^*,I_p^*,I_n^*,A_{pp}^*,A_{pn}^*,A^*)$, now, by extending this to t_{n+1} and replacing $\Phi^n=(S_p^{*n},S_n^{*n},I_p^{*n},I_n^{*n},A_{pp}^{*n},A_{pn}^{*n},A^{*n})$ we have

$$
\begin{aligned}
S_p^{*n+1} =& S_p^{*0} + \frac{\varrho t_n^{\varrho-1}(1-\omega)}{ABC(\omega)} f_1(t_n, \Phi^n) \\
&+ \frac{\omega\varrho}{ABC(\omega)\Gamma(\omega)} \int_0^{t_{n+1}} \tau^{\varrho-1}(t_{n+1}-\tau)^{\omega-1} f_1(\tau, \Phi^n)d\tau, \\
S_n^{*n+1} =& S_n^{*0} + \frac{\varrho t_n^{\varrho-1}(1-\omega)}{ABC(\omega)} f_2(t_n, \Phi^n) \\
&+ \frac{\omega\varrho}{ABC(\omega)\Gamma(\omega)} \int_0^{t_{n+1}} r^{\varrho-1}(t_{n+1}-\tau)^{\omega-1} f_2(\tau, \Phi^n)d\tau, \\
I_p^{*n+1} =& I_p^{*0} + \frac{\varrho t_n^{\varrho-1}(1-\omega)}{ABC(\omega)} f_3(t_n, \Phi^n) \\
&+ \frac{\omega\varrho}{ABC(\omega)\Gamma(\omega)} \int_0^{t_{n+1}} r^{\varrho-1}(t_{n+1}-\tau)^{\omega-1} f_3(\tau, \Phi^n)d\tau, \\
I_n^{*n+1} =& I_n^{*0} + \frac{\varrho t_n^{\varrho-1}(1-\omega)}{ABC(\omega)} f_4(t_n, \Phi^n) \\
&+ \frac{\omega\varrho}{ABC(\omega)\Gamma(\omega)} \int_0^{t_{n+1}} \tau^{\varrho-1}(t-\tau)^{\omega-1} f_4(\tau, \Phi^n)d\tau, \\
A_{pp}^{*n+1} =& A_{pp}^{*0} + \frac{\varrho t_n^{\varrho-1}(1-\omega)}{ABC(\omega)} f_5(t_n, \Phi^n) \\
&+ \frac{\omega\varrho}{ABC(\omega)\Gamma(\omega)} \int_0^{t_{n+1}} \tau^{\varrho-1}(t_{n+1}-\tau)^{\omega-1} f_5(\tau, \Phi)d\tau, \\
A_{pn}^{*n+1} =& A_{pn}^{*0} + \frac{\varrho t_n^{\varrho-1}(1-\omega)}{ABC(\omega)} f_6(t_n, \Phi^n) \\
&+ \frac{\omega\varrho}{ABC(\omega)\Gamma(\omega)} \int_0^{t_{n+1}} \tau^{\varrho-1}(t_{n+1}-\tau)^{\omega-1} f_6(\tau, \Phi^n)d\tau, \\
A^{*n+1} =& A^{*0} + \frac{\varrho t_n^{\varrho-1}(1-\omega)}{ABC(\omega)} f_7(t_n, \Phi^n) \\
&+ \frac{\omega\varrho}{ABC(\omega)\Gamma(\omega)} \int_0^{t_{n+1}} \tau^{\varrho-1}(t_{n+1}-\tau)^{\omega-1} f_7(\tau, \Phi^n)d\tau.
\end{aligned}
\tag{3.7}
$$

By using integral approximations, the above system can be expressed as follows:

$$\begin{aligned}
S_p^{*n+1} =& S_p^{*0} + \frac{\varrho t_n^{\varrho-1}(1-\omega)}{ABC(\omega)} f_1(t_n, \Phi^n) \\
&+ \frac{\omega\varrho}{ABC(\omega)\Gamma(\omega)} \sum_{j=0}^{n} \int_{t_j}^{t_{j+1}} \tau^{\varrho-1}(t_{n+1}-\tau)^{\omega-1} f_1(\tau, \Phi^n) d\tau, \\
S_n^{*n+1} =& S_n^{*0} + \frac{\varrho t_n^{\varrho-1}(1-\omega)}{ABC(\omega)} f_2(t_n, \Phi^n) \\
&+ \frac{\omega\varrho}{ABC(\omega)\Gamma(\omega)} \sum_{j=0}^{n} \int_{t_j}^{t_{j+1}} \tau^{\varrho-1}(t_{n+1}-\tau)^{\omega-1} f_2(\tau, \Phi^n) d\tau, \\
I_p^{*n+1} =& I_p^{*0} + \frac{\varrho t_n^{\varrho-1}(1-\omega)}{ABC(\omega)} f_3(t_n, \Phi^n) \\
&+ \frac{\omega\varrho}{ABC(\omega)\Gamma(\omega)} \sum_{j=0}^{n} \int_{t_j}^{t_{j+1}} r^{\varrho-1}(t_{n+1}-\tau)^{\omega-1} f_3(\tau, \Phi^n) d\tau, \\
I_n^{*n+1} =& I_n^{*0} + \frac{\varrho t_n^{\varrho-1}(1-\omega)}{ABC(\omega)} f_4(t_n, \Phi^n) \\
&+ \frac{\omega\varrho}{ABC(\omega)\Gamma(\omega)} \sum_{j=0}^{n} \int_{t_j}^{t_{j+1}} \tau^{\varrho-1}(t_{n+1}-\tau)^{\omega-1} f_4(\tau, \Phi^n) d\tau, \\
A_{pp}^{*n+1} =& A_{pp}^{*0} + \frac{\varrho t_n^{\varrho-1}(1-\omega)}{ABC(\omega)} f_5(t_n, \Phi^n) \\
&+ \frac{\omega\varrho}{ABC(\omega)\Gamma(\omega)} \sum_{j=0}^{n} \int_{t_j}^{t_{j+1}} \tau^{\varrho-1}(t_{n+1}-\tau)^{\omega-1} f_5(\tau, \Phi^n) d\tau, \\
A_{pn}^{*n+1} =& A_{pn}^{*0} + \frac{\varrho t_n^{\varrho-1}(1-\omega)}{ABC(\omega)} f_6(t_n, \Phi^n) \\
&+ \frac{\omega\varrho}{ABC(\omega)\Gamma(\omega)} \sum_{j=0}^{n} \int_{t_j}^{t_{j+1}} \tau^{\varrho-1}(t_{n+1}-\tau)^{\omega-1} f_6(\tau, \Phi^n) d\tau, \\
A^{*n+1} =& A^{*0} + \frac{\varrho t_n^{\varrho-1}(1-\omega)}{ABC(\omega)} f_7(t_n, \Phi^n) \\
&+ \frac{\omega\varrho}{ABC(\omega)\Gamma(\omega)} \sum_{j=0}^{n} \int_{t_j}^{t_{j+1}} \tau^{\varrho-1}(t_{n+1}-\tau)^{\omega-1} f_7(\tau, \Phi^n) d\tau.
\end{aligned} \tag{3.8}$$

By approximating $\tau^{\varrho-1} f_i(\Phi, \tau)$ in (t_j, t_{j+1}) and using the Lagrange interpolation technique, we have

$$
\begin{aligned}
S_p^{*n+1} &= S_p^{*0} + \frac{\varrho t_n^{\varrho-1}(1-\omega)}{ABC(\omega)} f_1(t_n,\Phi)+ \\
&\quad \frac{\varrho(\Delta t)^{\omega}}{ABC(\omega)\Gamma(\omega+2)} \sum_{j=0}^{n} [f_1(\Phi^j,t_j)*c1 - f_1(\Phi^{j-1},t_{j-1})*c2], \\
S_n^{*n+1} &= S_n^{*0} + \frac{\varrho t_n^{\varrho-1}(1-\omega)}{ABC(\omega)} f_2(t_n,\Phi)+ \\
&\quad \frac{\tau^*(\Delta t)^{\omega}}{ABC(\omega)\Gamma(\omega+2)} \sum_{j=0}^{n} [f_2(\Phi^j,t_j)*c1 - f_2(\Phi^{j-1},t_{j-1})*c2], \\
I_p^{*n+1} &= I_p^{*0} + \frac{\varrho t_n^{\varrho-1}(1-\omega)}{ABC(\omega)} f_3(t_n,\Phi)+ \\
&\quad \frac{\varrho(\Delta t)^{\omega}}{ABC(\omega)\Gamma(\omega+2)} \sum_{j=0}^{n} [f_3(\Phi^j,t_j)*c1 - f_3(\Phi^{j-1},t_{j-1})*c2], \\
I_n^{*n+1} &= I_n^{*0} + \frac{\varrho t_n^{\varrho-1}(1-\omega)}{ABC(\omega)} f_4(t_n,\Phi)+ \\
&\quad \frac{\varrho(\Delta t)^{\omega}}{ABC(\omega)\Gamma(\omega+2)} \sum_{j=0}^{n} [f_4(\Phi^j,t_j)*c1 - f_4(\Phi^{j-1},t_{j-1})*c2], \\
A_{pp}^{*n+1} &= A_{pp}^{0} + \frac{\varrho t_n^{\varrho-1}(1-\omega)}{ABC(\omega)} f_5(t_n,\Phi)+ \\
&\quad \frac{\tau^*(\Delta t)^{\omega}}{ABC(\omega)\Gamma(\omega+2)} \sum_{j=0}^{n} [f_5(\Phi^j,t_j)*c1 - f_5(\Phi^{j-1},t_{j-1})*c2], \\
A_{pn}^{*n+1} &= A_{pn}^{*0} + \frac{\varrho t_n^{\varrho-1}(1-\omega)}{ABC(\omega)} f_6(t_n,\Phi)+ \\
&\quad \frac{\varrho(\Delta t)^{\omega}}{ABC(\omega)\Gamma(\omega+2)} \sum_{j=0}^{n} [f_6(\Phi^j,t_j)*c1 - f_6(\Phi^{j-1},t_{j-1})*c2], \\
A^{*n+1} &= A^{*0} + \frac{\varrho t_n^{\varrho-1}(1-\omega)}{ABC(\omega)} f_7(t_n,\Phi)+ \\
&\quad \frac{\varrho(\Delta t)^{\omega}}{ABC(\omega)\Gamma(\omega+2)} \sum_{j=0}^{n} [f_7(\Phi^j,t_j)*c1 - f_7(\Phi^{j-1},t_{j-1})*c2], \\
c_1 &= t_j^{\varrho-1}((n+1-j)^{\omega}(n-j+2+\omega) - (n-j)^{\omega}(n-j+2+2\omega)), \\
c_2 &= t_{j-1}^{\varrho-1}((n-j+1)^{\omega+1} - (n-j)^{\omega}(n-j+1+\omega)).
\end{aligned}
\tag{3.9}
$$

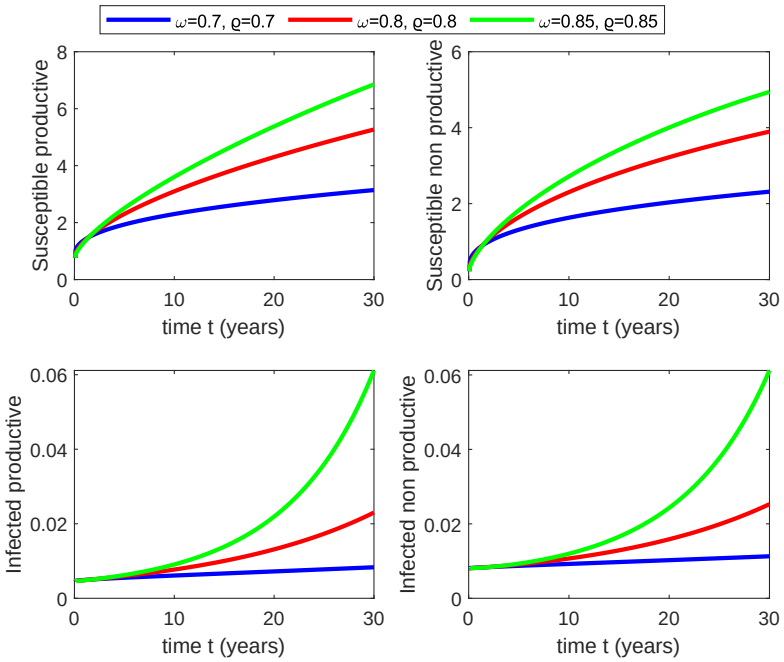

Figure 8. Fractal-fractional solution of the model for different values of ϱ and ω

The solution of the fractal-fractional-order model depends on the fractal dimension ϱ and the fractional order ω. As shown in Figure 8, as the fractal-fractional-order derivative decreased, the susceptible population decreased. Hence, the fractal-fractional-order is a better representation of the real problem of HIV/AIDS infection.

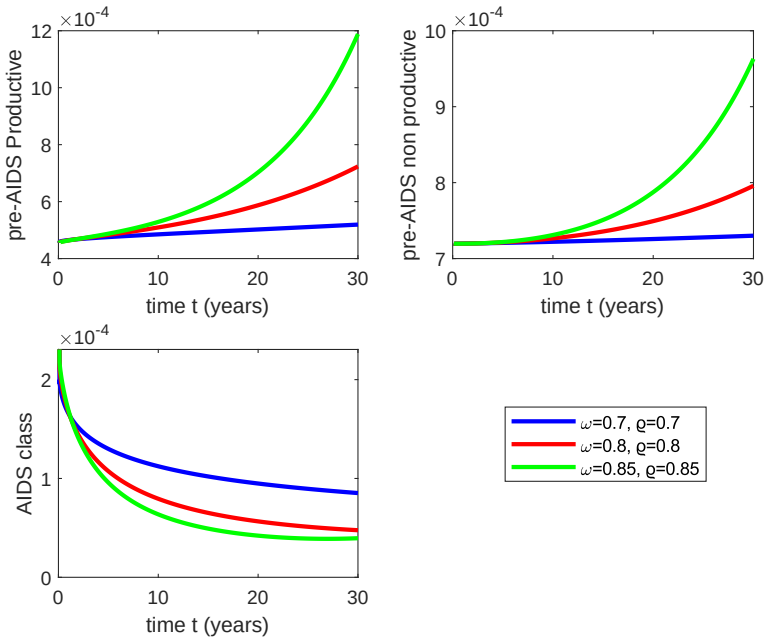

Figure 9. Fractal-fractional solution of the model for different values of ϱ and ω

In Figure 9, the graph of pre-AIDS productive and non-productive individuals increases rapidly for $\omega = 0.85$, and $\varrho = 0.85$, which is relatively unrealistic. The AIDS class population immediately approaches zero for $\omega = 0.85$ and $\varrho = 0.85$, and as we decrease the fractional order value, the AIDS class population slowly approaches zero.

3.3.1. Effect of the contact rate for fractal-fractional model version

A small change in the contact rate (β^*) changes the number of infected individuals. These values are directly proportional to the class of the infected population. Therefore, reducing the contact rate will decrease the number of people infected with HIV/AIDS.

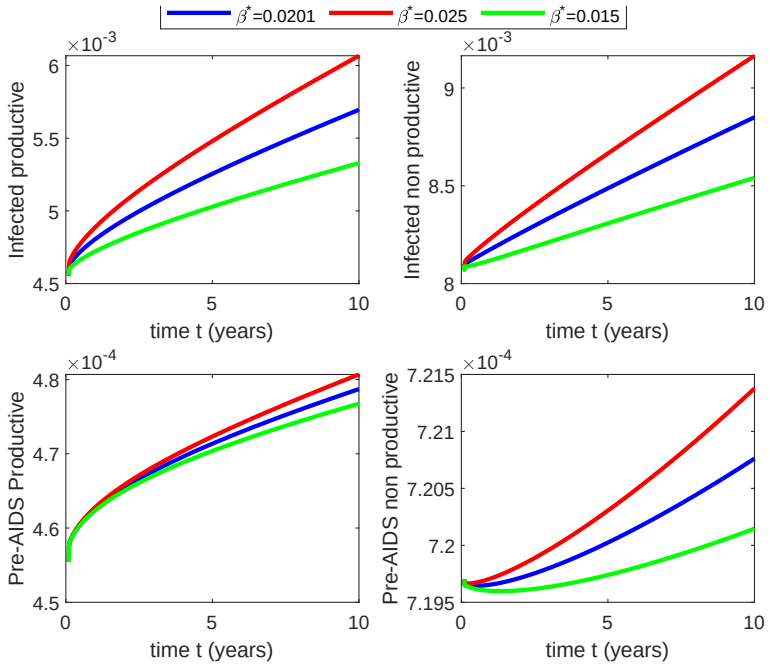

Figure 10. Effect contact rate if the fractal dimension($\varrho = 0.6$) and fractional order ($\omega = 0.8$)

The value of $\beta^* = 0.0201$ is the fitted value in Table 1, and we test for β^* below and above this value. According to Figure 10, a decreasing contact rate decreases the infected population and increases the susceptible population class. Similarly, the pre-AIDS productive and nonproductive classes.

3.3.2. Effect of the productivity rate

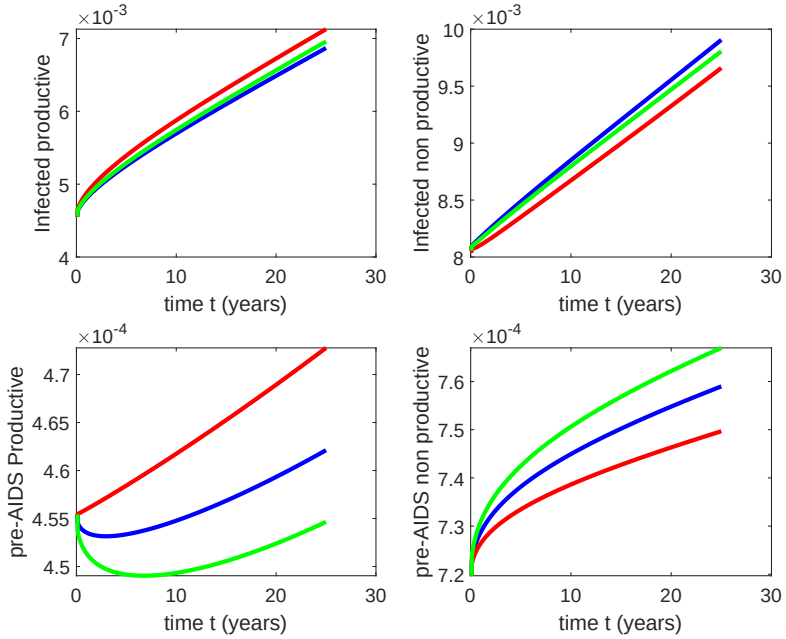

Figure 11. The effect of changing the rate of reducing the nonproductive population

Red line($\sigma_1^* = 0.02, \theta^* = 0.0012, \sigma_2^* = 0.02$) ,blue line($\sigma_1^* = 0.01, \theta^* = 0.01, \sigma_2^* = 0.015$), green line ($\sigma_1^* = 0.028, \theta^* = 0.003, \sigma_2^* = 0.025$) and ($\varrho = 0.6, \omega = 0.8$). As shown in Figure 11, increasing the rate of the active population in economic activity is used to increase the number of productive classes of the population regardless of their infection; they continue their normal lifestyle and reduce inequality due to HIV/AIDS infection.

4. Optimal control model

4.1. Extending the fractal-fractional order of the HIV/AIDS model to optimal control

Here, we extend Equation (2.2) to the optimal control model of fractal-fractional order of the HIV/AIDS model based on working-class populations. We consider the influence of the control variable $u_i(t), i = 1, 2, 3$, which varies from 0 to 1. A lack of control $u_i(t) = 0$ indicates no control intervention while achieving complete control $u_i(t) = 1$ is infeasible for certain constraints. The use of intervention measures is demonstrated by intermediate $u_i(t)$ values that fall within the interval of (0, 1). By incorporating the control variable into this model, we aim to reduce the proportion of individuals infected with HIV, non-productive, and fully diagnosed with AIDS. By incorporating the control variable, the model was updated from Equation (2.2) to Equation (4.1).

$$
\begin{aligned}
{}^{ABF}D_{0,t}^{\omega,\varrho}S_p^* &= \pi^*Q^* + \sigma_1^*(u_3+1)S_n^* - (\Lambda_c+\kappa)S_p^*,\\
{}^{ABF}D_{0,t}^{\omega,\varrho}S_n^* &= (1-\pi^*)Q^* - (\tau^*\Lambda_c + \sigma_1^*(u_3+1)+\kappa)S_n^*,\\
{}^{ABF}D_{0,t}^{\omega,\varrho}I_p^* &= \Lambda_c S_p^* + \theta^*(u_3+1)I_n^* - (\delta_1^*(1-u_2)+\kappa)I_p^*,\\
{}^{ABF}D_{0,t}^{\omega,\varrho}I_n^* &= \tau^*\Lambda_c S_n^* - (\theta^*(u_3+1)+\delta_2^*(1-u_2)+\kappa)I_n^*,\\
{}^{ABF}D_{0,t}^{\omega,\varrho}A_{pp}^* &= \delta_1^*(1-u_2)I_p^* + \sigma_2^*(u_3+1)A_{pn}^* - (k_1^*(1-u_2)+\kappa)A_{pp}^*,\\
{}^{ABF}D_{0,t}^{\omega,\varrho}A_{pn}^* &= \delta_2^*(1-u_2)I_n^* - (\sigma_2^*(u_3+1)+(k_2^*(1-u_2)+\kappa)A_{pn}^*,\\
{}^{ABF}D_{0,t}^{\omega,\varrho}A^* &= (k_1^*A_{pp}^* + k_2^*A_{pn}^*)(1-u_2) - (\kappa+\psi^*)A^*.
\end{aligned}
\tag{4.1}
$$

Within the force of infection, $\Lambda_c = \dfrac{\beta^*(I_p^*+I_n^*+A_{pp}^*+A_{pn}^*)}{N} * (1-u_1) = (1-u_1)\Lambda$ the initial condition $S_p^*(0) > 0, S_n^*(0) > 0, I_p^*(0) > 0, I_n^*(0) > 0, A_{pp}^*(0) > 0, A_{pn}^*(0) > 0, A^*(0) > 0$; all initial values are positive.

The major objective is to minimize the number of HIV-positive individuals in the selected population class. The cost incurred by interventions, where $u_i(t), i = 1,2,3$, are the control variables. To choose the best control unit, we define $u_1(t)$ as preventive control, $u_2(t)$ as ART treatment, and $u_3(t)$ as a special effort to reduce nonproductivity. We define the objective function ($\mathbf{J}$) with this goal.

$$
\mathbf{J}(u_1,u_2,u_3) = \min_{u_1,u_2,u_3}\int_0^{t_f}(b_1S_n^*+b_2I_p^*+b_3I_n^*+b_4A_{pp}^*+b_5A_{pn}^*+c_1u_1^2+c_2u_2^2+c_3u_3^2)dt,
\tag{4.2}
$$

where c_1, c_2, and c_3 are positive and represent the cost coefficients of the control measures u_i, the non-negative weights associated with the state variables b_i, and the final intervention time t_f. The optimal control problem involves identifying control functions u^* that minimize the objective function, considering the state system and constraints on the control variables, such as:

$$
\mathbf{J}(u^*) = minJ(u)|u = (u_1,u_2,u_3) \in \mathsf{A}.
\tag{4.3}
$$

$\mathsf{A} = \{(u_1,u_2,u_3)|u_i(t)$ is Lebsgue messurable with $0 \le u_i(t) \le 1, t \in [0,t_f], i = 1,2,3\}$ is the closed set, and $\mathbf{A}$ is the admissible control set, where, $u_{i,Max}$ are positive constants that represent the maximum values of the control measures [61,62]. The optimum control problem can be resolved by applying Pontryagin's principle, which asserts that adjoint variables $\lambda_i(t)$ exist and satisfy the optimality conditions of the Hamiltonian function Pontryagin [63].

$$
H = \frac{d\mathbf{J}(u^*)}{dt} + \lambda_1\frac{dS_p^*}{dt} + \lambda_2\frac{dS_n^*}{dt} + \lambda_3\frac{dI_p^*}{dt} + \lambda\frac{dI_n^*}{dt} + \lambda_5\frac{dA_{pp}^*}{dt} + \lambda_6\frac{dA_{pn}^*}{dt} + \lambda_7\frac{dA^*}{dt},
$$

The system minimizes the related costate variables with state variables $S_p^*, S_n^*, I_p^*, I_n^*, A_{pp}^*, A_{pn}^*$ and A^* at each time t, thereby satisfying the differential equation system Mondal and Khajanchi [64].

$$
\frac{d\lambda_1}{dt} = \frac{-\partial H}{\partial S_p^*}, \frac{d\lambda_2}{dt} = \frac{-\partial H}{\partial S_n^*}, \frac{d\lambda_3}{dt} = \frac{-\partial H}{\partial I_p^*}, \frac{d\lambda_4}{dt} = \frac{-\partial H}{\partial I_n^*}, \frac{d\lambda_5}{dt} = \frac{-\partial H}{\partial A_{pp}^*},
$$

$\dfrac{d\lambda_6}{dt} = \dfrac{-\partial H}{\partial A_{pn}^*}, \dfrac{d\lambda_7}{dt} = \dfrac{-\partial H}{\partial A^*}$ and $\Lambda_c = \dfrac{\beta^*(I_p^*+I_n^*+A_{pp}^*+A_{pn}^*)}{N} * (1-u_1)$, assume

N scaled to 1. Then,

$$\begin{aligned}
\frac{d\lambda_1}{dt} =&(\lambda_1-\lambda_3)(I_p^*+I_n^*+A_{pp}^*+A_{pn}^*)(1-u1)+\lambda_1\kappa,\\
\frac{d\lambda_2}{dt} =&(\lambda_2-\lambda_4)\tau^*(I_p+I_n^*+A_{pp}^*+A_{pn}^*)*(1-u_1)-\lambda_1\sigma_1^*(u_3+1)-\lambda_2\kappa-b_1,\\
\frac{d\lambda_3}{dt} =&(\lambda_2-\lambda_4)(1-u_1)\tau^*\beta^*S_n^*+(\lambda_1-\lambda_3)(1-u_1)\beta^*S_p^*-(\lambda_3+\lambda_5)\delta_1^*(1-u_1)\\
&-\lambda_3\kappa-b_2,\\
\frac{d\lambda_4}{dt} =&(\lambda_1-\lambda_3)(1-u_1)\beta^*S_p^*+(\lambda_2-\lambda_4)(1-u_1)\tau^*\beta^*S_n^*+(\lambda_4-\lambda_3)\theta^*(u_3+1)+\\
&(\lambda_4-\lambda_6)\delta_2^*(1-u_2)+\lambda_4\kappa-b_3,\\
\frac{d\lambda 5}{dt} =&(\lambda_1-\lambda_3)(1-u_1)\beta^*S_p^*+(\lambda_2-\lambda_4)\tau^*(1-u_1)\beta^*S_n^*+(\lambda_5-\lambda_7)k_1^*(1-u_2)\\
&+\lambda_5\kappa-b_4,\\
\frac{d\lambda 6}{dt} =&(\lambda_1-\lambda_3)\beta^*(1-u_1)\beta^*S_p^*+(\lambda_2-\lambda_4)\beta^*\tau^*(1-u_1)S_n+(\lambda_6-\lambda_5)\sigma_2^*(u_3+1),\\
&+(\lambda_6-\lambda_7)k_2^*(1-u_2)+\lambda_6\kappa-b_5,\\
\frac{d\lambda 7}{dt} =&\lambda_7(\kappa+\psi^*),
\end{aligned} \tag{4.4}$$

with transversality conditions:

$$\lambda_i(T)=0,\quad i=1,\dots,7.$$

Now drive the optimal control functions

$$\begin{aligned}
\frac{\partial H}{\partial u_1} &= 2c_1u_1+(\lambda_1-\lambda_3)\Lambda S_p^*+(\lambda_2-\lambda_4)\tau^*\Lambda S_n^*=0,\\
\frac{\partial H}{\partial u_2} &= 2c_2u_2+(\lambda_4-\lambda_6)\delta_2^*I_n^*+(\lambda_6-\lambda_7)k_2A_{pn}^*+(\lambda_5-\lambda_7)k_1A_{pp}^*-\lambda_5\delta_1^*I_P^*=0,\\
\frac{\partial H}{\partial u_3} &= 2c_3u_3+(\lambda_2-\lambda_1)\sigma_1^*S_n^*+(\lambda_4-\lambda_3)\theta^*I_n^*+(\lambda_6-\lambda_5)\sigma_2^*A_{pn}=0.
\end{aligned} \tag{4.5}$$

From this system, we solve for the optimal control function u_1, u_2, and u_3,

$$\begin{aligned}
u_1 &= \frac{(\lambda_3-\lambda_1)\Lambda S_p^*+(\lambda_4-\lambda_2)\tau^*\Lambda S_n^*}{2c_1},\\
u_2 &= \frac{(\lambda_6-\lambda_4)\delta_2^*I_n^*+(\lambda_7-\lambda_6)k_2^*A_{pn}^*+(\lambda_7-\lambda_5)k_1^*A_{pp}^*+\lambda_5\delta_1^*I_p^*}{2c_2},\\
u_3 &= \frac{(\lambda_2-\lambda_3)\sigma_1^*S_n^*+(\lambda_4-\lambda_3)\theta^*I_n^*+(\lambda_6-\lambda_5)\sigma_2^*A_{pn}^*}{2c_3},\\
u^*(t) &= \min\left[\max\left(0,u_1,u_2,u_3\right),1\right].
\end{aligned} \tag{4.6}$$

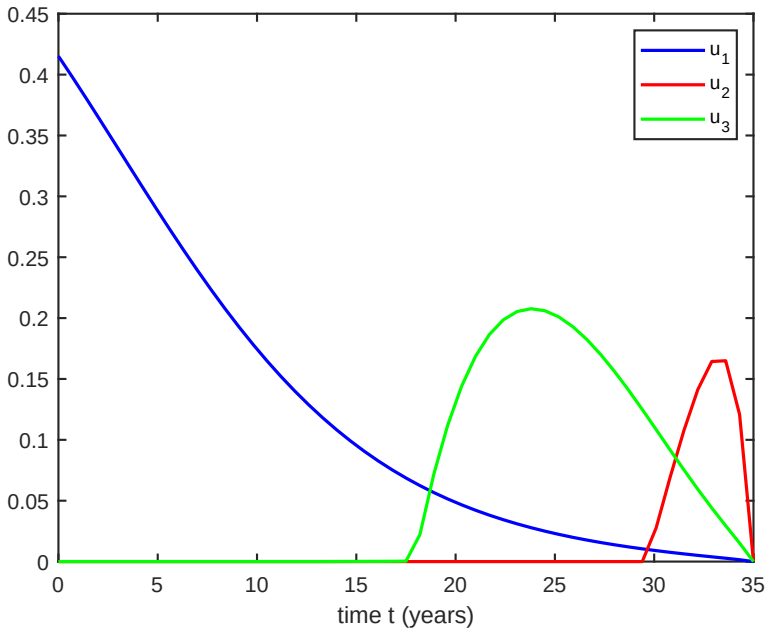

Figure 12. Optimal Control Function

4.2. Simulation of fractal-fractional optimal control solutions

The numerical simulation shows that using all strategies at the same time gives better results in combating the spread of HIV/AIDS and reducing the nonproductive population both in susceptible and infected populations. Based on this result, we discuss only the option to use all strategies at the same time.

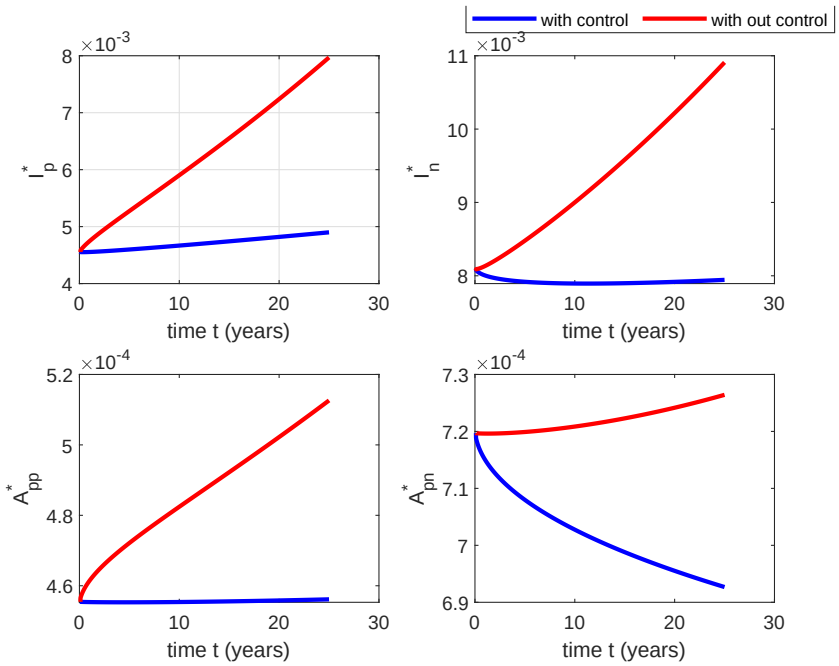

Figure 13. The effect of optimal control on each compartment

As shown in Figure 13, optimal control is applied to increase the productive population and decrease the nonproductive population after infection.

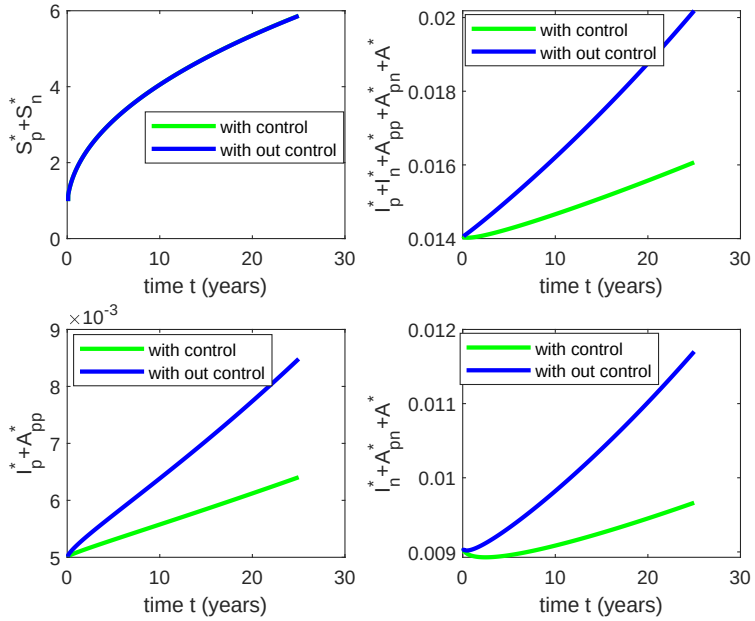

Figure 14. Total susceptible, infected productive, infected nonproductive population with control and without control

When we applied the control variable to the model, as shown in Figure 14, the total infected population decreased with the control and increased without the control, but the total infected population in both the productive and nonproductive infected populations decreased. This means that when we apply the control intervention, the total susceptible population increases and the infected population increases. In addition, after they are infected, the productive class population remains in the productive class for a long time.

5. Conclusion

In this study, the researchers formulated a fractal-fractional order mathematical model to analyze the effect of HIV/AIDS on the working-class population in Ethiopia. The researchers used the Atangana-Baleanu fractional operator following the Caputo operator as the basis for the model. The fractal-fractional model was further extended to an optimal control model to apply control strategies and study the impact of HIV/AIDS on the working-class. Banach's fixed-point theorem and Contraction principle are used by the researchers to demonstrate the existence and uniqueness of a solution to the model. It is also shown that the model is stable based on Hyers-Ulam stability analysis. The researchers calculated the disease-free and endemic equilibrium points and used the next-generation matrix to determine the reproduction number. The reproduction number values are found to be less than one for the disease-free equilibrium points, which are asymptotically stable.

Fractional-order mathematical model to analyze the effect of HIV/AIDS on the working-class is solved by using numerical methods. The simulations were

performed using MATLAB R2020a. The cases of integral, fractional, and fractal-fractional-order models were solved, and the fractal-fractional-order model was more realistic and represented the real system accurately. The model was fitted to Model (2.1) using 23 years of data. The solution of the fractional order for different orders of derivatives was simulated to show the difference between the integral and fractional-order models, as shown in Figures 6 and 7. This model has the property of an integral model if the order of the derivative $\omega = 1$. In Figures 8 and 9, we simulate a fractal-fractional model for different values of fractional order and fractal dimension. From this, we understand that the fractal-fractional order model is better than the integral and fractional-order models in representing the dynamics of HIV/AIDS infection in the working-class. The fractal-fractional version of the model is discussed using the contact rate β^*, reducing the value of β^* decreases the number of people infected by HIV/AIDS, as shown in Figure 10. Therefore, reducing the contact rate between infected and susceptible populations is important for mitigating the spread and transmission of HIV. Again, simulations were performed on the parameters used to reduce the rate of nonproductivity, as shown in Figure 11. Reducing the number of people in the nonproductivity class increases the number of people in the productive class, which is important because it reduces the identified barriers to ending HIV/AIDS, such as discrimination and inequality. This condition can be supported by appropriate ART treatment and awareness creation using various methods.

In addition, the researcher has extended the model to an optimal control problem and numerical simulations, as shown in Figures 13 and 14. Different control measures are applied to increase the productive population class and decrease the nonproductive population class after infection. Concerning the solutions related to the deterministic HIV/AIDS model, fractional and fractal-fractional-order HIV/AIDS epidemic models have shown that the fractal-fractional model is more realistic than the deterministic and fractional models. For further study, an extension of this work depends on piecewise mathematical modeling.

Declaration of competing interests

The authors declare that none of their known financial conflicts or interpersonal connections could have biased this study.

References

[1] P. J. Kanki and C. K. Koofhethile, Hiv/aids global epidemic, in Infectious Diseases, Springer, 2023, 221-250.

[2] M. Arefaynie, Y. Damtie, B. Kefale and M. Yalew, Predictors of discrimination towards people living with hiv/aids among people aged 15–49 years in ethiopia: a multilevel analysis, HIV/AIDS-Research and Palliative Care, 2021, 283-292.

[3] Y. Shiferaw, A. Alemu, A. Girma et al., Assessment of knowledge, attitude and risk behaviors towards hiv/aids and other sexual transmitted infection among preparatory students of gondar town, north west ethiopia, BMC research notes, 2011, 4, 1-8.

[4] WHO, Preventing and addressing abusive conduct, 2023, https://www.who.int/news-room/fact-sheets/detail/hiv-aids

[5] UNAIDS, Latest global and regional hiv statistics on the status of the aids epidemic accessed on 9/29/2024, 2024.

[6] F. T. Nigusso and A. H. Mavhandu-Mudzusi, Health-related quality of life of people living with hiv/aids: the role of social inequalities and disease-related factors, Health and Quality of Life Outcomes, 2021, 19, 1-11.

[7] G. K. Nikolopoulos and A. G. Tsantes, Recent hiv infection: Diagnosis and public health implications, Diagnostics, 2022, 12(11), 2657.

[8] M.Adal, Systematic review on HIV , situation in Addis Ababa, Ethiopia. BMC Public Health 19, 1544 (2019).
DOI: org/10.1186/s12889-019-7885-8.

[9] Y. Luchko, Fractional derivatives and the fundamental theorem of fractional calculus, Fractional Calculus and Applied Analysis, 2020, 23(4), 939-966.

[10] I. Podlubny, An introduction to fractional derivatives, fractional differential equations, to methods of their solution and some of their applications, Math. Sci. Eng, 1999, 198(340), 0924-34008.

[11] M. Abu-Ghuwaleh and R. Saadeh, New definitions of fractional derivatives and integrals for complex analytic functions, Arab Journal of Basic and Applied Sciences, 2023, 30(1), 675-690.

[12] A. Atangana, Extension of rate of change concept: from local to nonlocal operators with applications, Results in Physics, 2020, 19, 103515.

[13] S. Ahmed, S. Jahan and K. S. Nisar, Hybrid fibonacci wavelet method to solve fractional-order logistic growth model, Mathematical Methods in the Applied Sciences, 2023, 46(15), 16218-16231.

[14] T. M. Rassias, Functional equations in mathematical analysis,Springer, 2012.

[15] A. E. Sado and B. S. Kotola, A mathematical model based on ABC fractional order for TB transmission with treatment interruptions in case of bule hora town, ethiopia, Informatics in Medicine Unlocked, 2024.
DOI: 10.1016/j.imu.2024.101498.

[16] P. Yadav, S. Jahan, K. Shah et al., Fractional-order modelling and analysis of diabetes mellitus: Utilizing the Atangana-Baleanu Caputo (ABC) operator, Alexandria Engineering Journal, 2023, 81, 200-209.

[17] S. Ahmed, S. Jahan, K. Shah and T. Abdeljawad, On mathematical modelling of measles disease via collocation approach, AIMS Public Health, 2024, 11(2), 628-653.

[18] J. Gómez-Aguilar and A. Atangana, New chaotic attractors: Application of fractal-fractional differentiation and integration, Mathematical Methods in the Applied Sciences, 2021, 44(4), 3036-3065.

[19] A. Atangana, Fractal-fractional differentiation and integration: connecting fractal calculus and fractional calculus to predict complex system, Chaos, solitons & fractals, 2017, 102, 396-406.

[20] S. Kumar, R. Kumar, J. Singh et al., An efficient numerical scheme for fractional model of hiv-1 infection of cd4+ t-cells with the effect of antiviral drug therapy, Alexandria Engineering Journal, 2020, 59(4), 2053-2064.

[21] L. Sadek, O. Sadek, H. T. Alaoui et al., Fractional order modeling of predicting covid-19 with isolation and vaccination strategies in morocco, CMES-Comput. Model. Eng. Sci, 2023, 136, 1931-1950.

[22] K. Shah and T. Abdeljawad, Study of a mathematical model of covid-19 outbreak using some advanced analysis, Waves in random and complex media, 2022, 1-18.

[23] W. Shatanawi, M. S. Abdo, M. A. Abdulwasaa et al., A fractional dynamics of tuberculosis (tb) model in the frame of generalized atangana–baleanu derivative, Results in Physics, 2021, 29, 104739.

[24] K. M. Saad, M. Alqhtani and J. Gómez-Aguilar, Fractal-fractional study of the hepatitis c virus infection model, Results in Physics, 2020, 19, 103555.

[25] B. Ghanbari and J. Gómez-Aguilar, Analysis of two avian influenza epidemic models involving fractal-fractional derivatives with power and mittag-leffler memories, Chaos: An Interdisciplinary Journal of Nonlinear Science, 2019, 29(12).

[26] A. K. Gizaw and C. T. Deressa, Analysis of age-structured mathematical model of malaria transmission dynamics via classical and abc fractional operators, Mathematical Problems in Engineering, 2024, 2024(1), 3855146.

[27] J. Gomez-Aguilar, T. Cordova-Fraga, T. Abdeljawad et al., Analysis of fractal–fractional malaria transmission model, Fractals, 2020, 28(08), 2040041.

[28] P. A. Naik, M. Farman, A. Zehra et al., Analysis and modeling with fractal-fractional operator for an epidemic model with reference to covid-19 modeling, Partial Differential Equations in Applied Mathematics, 2024, 10, 100663.

[29] K. S. Nisar and Y. Sabbar, Long-run analysis of a perturbed hiv/aids model with antiretroviral therapy and heavy-tailed increments performed by tempered stable lévy jumps, Alexandria Engineering Journal, 2023, 78, 498-516.

[30] A. Shaikh, K. S. Nisar, V. Jadhav et al., Dynamical behaviour of hiv/aids model using fractional derivative with mittag-leffler kernel, Alexandria Engineering Journal, 2022, 61(4), 2601-2610.

[31] P. Yadav, S. Jahan and M. Izadi, Taylor wavelet quasilinearization method for solving tumor growth model of fractional order, Results in Control and Optimization, 2024.
DOI: 10.1016/j.rico.2024.100437.

[32] P. Yadav, S. Jahan and K. S. Nisar, Analysis of fractal-fractional alzheimer's disease mathematical model in sense of caputo derivative, AIMS Public Health, 2024, 11(2), 399-419.

[33] K. A. Abro, A. Atangana and J. Gomez-Aguilar,Ferromagnetic chaos in thermal convection of fluid through fractal–fractional differentiations, Journal of Thermal Analysis and Calorimetry, 2022, 147(15), 8461-8473.

[34] K. A. Abro, A. Atangana and J. Gómez-Aguilar, Chaos control and characterization of brushless dc motor via integral and differential fractal-fractional techniques, International Journal of Modelling and Simulation, 2023, 43(4), 416-425.

[35] C. T. Deressa, S. Etemad and S. Rezapour, On a new four-dimensional model of memristor-based chaotic circuit in the context of nonsingular atangana–baleanu–caputo operators, Advances in difference equations, 2021, 2021, 1-24.

[36] S. Jahan, S. Ahmed, P. Yadav and K. S. Nisar, Fibonacci wavelet method for the numerical solution of a fractional relaxation–oscillation model, Partial Differential Equations in Applied Mathematics, 2023, 8, 100568.

[37] V. Vijayaraj, C. Ravichandran, K. S. Nisar et al., An outlook on the controllability of non-instantaneous impulsive neutral fractional nonlocal systems via atangana–baleanu–caputo derivative, Arab Journal of Basic and Applied Sciences, 2023, 30(1), 440-451.

[38] Z. U. A. Zafar, N. Ali, S. Younas et al., Numerical investigations of stochastic hiv/aids infection model, Alexandria Engineering Journal, 2021, 60(6), 5341-5363.

[39] C. Zúñiga-Aguilar, J. F. Gómez-Aguilar, H. Romero-Ugalde et al., Fractal-fractional neuro-adaptive method for system identification, Engineering with Computers, 2022, 38, 3085-3108.

[40] A. Khan, T. Abdeljawad and M. A. Alqudah, Neural networking study of worms in a wireless sensor model in the sense of fractal fractional, AIMS Mathematics, 2023, 8(11), 26406-26424.

[41] M. Toufik and A. Atangana, New numerical approximation of fractional derivative with non-local and non-singular kernel: application to chaotic models, The european physical journal plus, 2017, 132, 1-16.

[42] A. Atangana and S. Qureshi, Modeling attractors of chaotic dynamical systems with fractal–fractional operators, Chaos, solitons & fractals, 2019, 123, 320-337.

[43] A. Khan, K. Shah, T. Abdeljawad and I. Amacha, Fractal fractional model for tuberculosis: existence and numerical solutions, Scientific Reports, 2024, 14(1), 12211.

[44] P. Yadav, S. Jahan and K. S. Nisar, Fractional order mathematical model of ebola virus under atangana–baleanu–caputo operator, Results in Control and Optimization, 2023.
DOI: 10.1016/j.rico.2023.100332.

[45] B. Seidu and O. D. Makinde, Optimal control of hiv/aids in the workplace in the presence of careless individuals, Computational and mathematical methods in medicine, 2014.
DOI: 10.1155/2014/831506.

[46] Z. Ali, F. Rabiei, K. Shah and T. Khodadadi, Fractal-fractional order dynamical behavior of an hiv/aids epidemic mathematical model, The European Physical Journal Plus, 2021, 136(1), 36.

[47] Z. Ali, A. Zada and K. Shah, On ulam's stability for a coupled systems of nonlinear implicit fractional differential equations, Bulletin of the Malaysian Mathematical Sciences Society, 2019, 42, 2681-2699.

[48] R. Murali and A. P. Selvan, On the generalized hyers-ulam stability of linear ordinary differential equations of higher order, International Journal of Pure and Applied Mathematics, 2017, 117(12), 317-326.

[49] K. Shah, M. Sarwar, T. Abdeljawad et al., A comprehensive mathematical analysis of fractal–fractional order nonlinear re-infection model, Alexandria Engineering Journal, 2024, 103, 353-365.

[50] K. Shah, M. Sarwar, T. Abdeljawad et al., On mathematical model of infectious disease by using fractals fractional analysis, Discrete and Continuous Dynamical Systems-S, 2024, 0-0.

[51] P. Van den Driessche and J. Watmough, Reproduction numbers and subthreshold endemic equilibria for compartmental models of disease transmission, Mathematical biosciences, 2002, 180(1-2), 29-48.

[52] A. Atangana and S. İ. Araz, Nonlinear equations with global differential and integral operators: existence, uniqueness with application to epidemiology, Results in Physics, 2021, 20, 103593.

[53] T. Nabil, Krasnoselskii n-tupled fixed point theorem with applications to fractional nonlinear dynamical system, Advances in Mathematical Physics, 2019, 2019(1), 6763842.

[54] A. Atangana and S. İ. Araz, Extension of atangana-seda numerical method to partial differential equations with integer and non-integer order, Alexandria Engineering Journal, 2020, 59(4), 2355-2370.

[55] A. Boukhouima, E. M. Lotfi, M. Mahrouf et al., Stability analysis and optimal control of a fractional hiv-aids epidemic model with memory and general incidence rate, The European Physical Journal Plus, 2021, 136(1), 1-20.

[56] D. Baleanu and A. Fernandez, On some new properties of fractional derivatives with mittag-leffler kernel, Communications in Nonlinear Science and Numerical Simulation, 2018, 59, 444-462.

[57] A. Omame, M. Abbas and C. Onyenegecha, A fractional-order model for covid-19 and tuberculosis co-infection using atangana–baleanu derivative, Chaos, Solitons & Fractals, 2021, 153, 111486.

[58] C. Castillo-Chavez, On the computation of R_0. and its role on global stability carlos castillo-chavez, zhilan feng, and wenzhang huang, Mathematical approaches for emerging and reemerging infectious diseases: an introduction, 2002, 1, 229.

[59] J. R. Graef, C. Tunç, M. Şengun and O. Tunç, The stability of nonlinear delay integro-differential equations in the sense of hyers-ulam, Nonautonomous Dynamical Systems, 2023, 10(1), 20220169.

[60] C. T. Deressa and G. F. Duressa, Analysis of atangana–baleanu fractional-order seair epidemic model with optimal control, Advances in Difference Equations, 2021, 2021, 1-25.

[61] T. K. Ayele, E. F. D. Goufo and S. Mugisha, Mathematical modeling of hiv/aids with optimal control: a case study in ethiopia, Results in Physics, 2021, 26, 104263.

[62] K. R. Cheneke, Optimal control and bifurcation analysis of hiv model, Computational and Mathematical Methods in Medicine, 2023, 2023(1), 4754426.

[63] L. S. Pontryagin, Mathematical theory of optimal processes, Routledge, 2018.

[64] J. Mondal and S. Khajanchi, Mathematical modeling and optimal intervention strategies of the covid-19 outbreak, Nonlinear dynamics, 2022, 109(1), 177-202.